2008

Live load distribution factors for glued-laminated timber bridges

Jeremy James May
Iowa State University

Live load distribution factors for glued-laminated timber bridges

by

Jeremy James May

A thesis submitted to the graduate faculty

in partial fulfillment of the requirements for the degree of

MASTER OF SCIENCE

Major: Civil Engineering (Structural Engineering)

Program of Study Committee:
Fouad Fanous, Co-Major Professor
Terry J. Wipf, Co-Major Professor
Lester W. Schmerr

Iowa State University

Ames, Iowa

2008

TABLE OF CONTENTS

LIST OF FIGURES

LIST OF TABLES

ABSTRACT

Over the past years the United States Department of Agriculture - Forest Products Laboratory and the Federal Highway Administration have supported several research programs. This thesis is a result of a study sponsored by the Forest Products Laboratory, with the objective of determining how truckloads are distributed to the structural members of glued-laminated timber bridges. Glued-laminated timber girder bridges with glued-laminated timber deck panels and longitudinal glued-laminated timber deck bridges were the focus of this paper. Currently, the American Association of State Highway and Transportation Officials LRFD Bridge Design Specification provides live load distribution provisions for glued-laminated timber bridges. This paper investigates the existing live load distribution provisions for glued-laminated timber bridges utilizing field test data collected by Iowa State University researchers, laboratory test data, and analytical finite element modeling. From this data, simplified live load distribution equations were developed following methods established for other bridge types where needed to improve the accuracy of determining how truckloads are distributed to structural members of glued-laminated timber bridges.

CHAPTER 1. INTRODUCTION

Bridges in the United States are designed on procedures and specifications endorsed by the American Association of State Highway and Transportation Officials (AASHTO). Largely, these design specifications are based on performance data obtained from research and experience. Bridge design specifications must be revised on a regular basis to reflect new information, and revisions or modifications are introduced on a yearly basis. Timber bridge design procedures have been part of the AASHTO Bridge Design Specifications for many years. In the past several decades, ongoing research has provided the basis for many timber bridge design provisions. A significant amount of research data, particularly from field load tests, has yet to be used to assess the existing AASHTO timber bridge design specifications. In conjunction with the field test data, finite element analyses were performed to further evaluate the existing AASHTO design specifications on a broader range of bridges. The specific objective of the study presented herein is to determine how highway truck live loads are distributed on glued-laminated timber bridges. Modifications to the existing live load distribution provisions currently presented in the AASHTO LRFD Bridge Design Specifications were developed based on the field test and finite element results. This report is composed of two papers, both of which have been submitted for publication.

Chapter two of this thesis consists of the first paper, “Live Load Distribution On Glued Laminated Timber Girder Bridges.” This paper is committed to determining how highway truck loads are distributed to girders of a glued-laminated timber girder bridge with glued-laminated timber deck panels. This was accomplished utilizing field test data and finite element analysis data collected from a wide range of glued-laminated timber girder bridges. From the data above, the worst-case live load distribution factors that can be used to calculate the design moment and

shear for glued-laminated timber girders were used to evaluate the existing AASHTO LRFD live load distribution provisions and to create new live load distribution equations.

Chapter three of this paper consists of the second paper, “Live Load Distribution On Longitudinal Glued Laminated Timber Deck Bridges.” This paper is committed to determining how highway truck loads are distributed to deck panels of a longitudinal glued-laminated timber deck panel bridge. The AASHTO LRFD live load distribution provisions for longitudinal glued-laminated timber deck bridges were based on the assumption that the bridge deck behaves as one slab, i.e. ignoring the discontinuity of the bridge deck panels. This report investigates this assumption utilizing field test data, laboratory test data, and finite element analysis results.

CHAPTER 2. LIVE LOAD DISTRIBUTION ON GLUED LAMINATED TIMBER GIRDER BRIDGES

Abstract

The increased use of timber bridges in the United States transportation system has required additional research to improve the current design methodology of these bridges. For this reason, The United States Department of Agriculture (USDA) - Forest Products Laboratory (FPL) and the Federal Highway Administration (FHWA) have supported several research programs to attain the objective listed above. This report is a result of a study sponsored by the FPL, with the objective of determining how highway truckloads are distributed to girders of a glued-laminated timber bridge. The American Association of State Highway and Transportation Official (AASHTO) LRFD Bridge Design Specification provides live load distribution provisions for glued-laminated girder timber bridges, which were used in previous AASHTO specifications. The AASHTO live load distribution provisions were reviewed in this report.

Field test results were used to review the current AASHTO LRFD glued-laminated timber girder bridge design specifications and to validate analytical results obtained by finite element analyses. With the validated analytical models, parametric studies were performed to determine the worst-case live load distribution factors that can be used to calculate the design moment and shear for glued-laminated timber girders. Simplified live load distribution equations that can be utilized to determine these distribution factors were developed and are provided in this report. These equations take into account how load is distributed to the bridge girders considering the effects of span length, girder spacing, and clear width of the bridge.

Objective and scope

The overall objective of the study presented herein is to evaluate the live load distribution provisions provided in the 2005 AASHTO LRFD Bridge Design Specifications [2] in relation to glued-laminated timber bridges. In addition, recommendations and revisions to the AASHTO LRFD live load distribution provisions will be developed if required. The objectives listed above were accomplished by completing the following six tasks:

1. Review the current 2005 American Association of State Highway and Transportation Officials (AASHTO) LRFD Bridge Design Specifications and the associated load distribution criteria for glued-laminated timber girder bridges.
2. Develop detailed analytical finite element models to evaluate the structural performance of the glued-laminated timber bridges. These analytical models include the orthotropic behavior of timber material.
3. The analytical finite element models were validated by comparing the calculated analytical girder deflections and load distribution results to the data obtained from the field tests of the in-service bridges conducted by researchers at ISU.
4. Finite element analyses were conducted to determine the controlling live load distribution factors for the design shear and moment values in the bridge girders. This was necessary to investigate the influence of several geometric and material property parameters.
5. The analytical live load distribution results, for moment and shear, were then compared to the 2005 AASHTO LRFD live load distribution provisions.
6. Based on the comparison mentioned above, the AASHTO LRFD live load distribution provisions for glued-laminated timber girder bridges were revised to accurately represent the load distribution in these types of bridges

Background

Simple live load distribution equations have appeared in the AASHTO bridge design specifications for many years. However, the AASHTO LRFD bridge design specification introduced major revisions to the live load distribution provisions. Unfortunately, these revisions to the AASHTO LRFD live load distribution provisions did not incorporate similar distribution factors for glued-laminated timber girder bridges.

The 1996 AASHTO Standard Specification [1] live load distribution equations for glued-laminated timber girder bridges were presented based on wheel loads, or half of the total axle load. These equations are listed in Table 1 for an interior girder under single or multiple traffic lane loadings. The wheel load distribution factors in Table 1 include multiple presence factors. The same load distribution equation is used when calculating either the design moment or shear for a bridge girder.

Table 1. 1996 AASHTO Standard Specification, Wheel Load Distribution Factors [1]

Design Condition	One Traffic Lane	Two or More Traffic Lanes
Moment	S/6	S/5
Shear	S/6	S/5

Where:

S = Girder spacing (feet)

The 2005 AASHTO LRFD [2] live load distribution equations for glued laminated timber girder bridges were presented based on lane loads, or the total axle load. These equations are listed in Table 2 for an interior girder under single or multiple traffic lane loads. The lane load distribution factors in Table 2 include multiple presence factors. As can be seen, the same load distribution equation is used to determine the design moment and shear.

Table 2. 2005 AASHTO LRFD Design Specification, Lane Load Distribution Factors [2]

Design Condition	One Traffic Lane	Two or More Traffic Lanes
Moment	S/10	S/10
Shear	S/10	S/10

Where:

S = Girder spacing (feet)

As previously mentioned, multiple presence factors were included in the 1996 AASHTO Standard and 2005 AASHTO LRFD live load distribution provisions. Multiple presence factors account for the probability of several load combinations and are provided in Table 3. For bridges with multiple design lanes, it is unlikely three adjacent lanes will be loaded at the same time. Therefore, the design load is decreased. For the single design lane condition, the multiple presence factor in the AASHTO LRFD specification is greater than one to account for an overload condition. Multiple presence factors need to be applied to distribution factors determined using alternative analysis methods or simplified methods such as the lever rule.

Table 3. AASHTO Multiple Presence "m" Factors

Number of Loaded Lanes	Standard Specification [1]	2005 LRFD [2]
1	1.0	1.2
2	1.0	1.0
3	0.9	0.85
> 3	0.75	0.65

The 2005 AASHTO LRFD multiple presence factors were developed based on an average daily truck traffic (ADTT) value of 5,000 trucks in one direction. The 2005 AASHTO LRFD commentary, C3.6.1.1.2, allows the following adjustments to the multiple presence factors based on sites with lower ADTT values [2]:

- If $100 \leq ADTT \leq 1{,}000$, 95 percent of the specified force effect may be used.

- If ADTT < 100, 90 percent of the specified force effect may be used.

The AASHTO live load distribution equations presented in Table 1 and Table 2 remained essentially unchanged for interior girders. The live load distribution equations in the AASHTO LRFD specification, provided in Table 2, were attained by adjusting the AASHTO Standard specification equations, provided in Table 1, from wheel loads to lane loads and by incorporating the multiple presence factor changes. The transformations above were incorporated to the live load distribution equations for all bridge types in the AASHTO LRFD specification.

The distribution factors above are used for the design of interior glued-laminated timber girders. The live load distribution factors for exterior girders are determined using the lever rule. The lever rule method, for exterior girders, has remained unchanged from the 1996 AASHTO Standard Specification to the 2005 AASHTO LRFD Specification. The lever rule assumes the girders to act as rigid supports to the bridge deck. In addition, the lever rule neglects continuity of the bridge deck over the interior girders by introducing hinges at the deck-girder connection, as shown in Figure 1. Therefore, the second wheel load located between girders G2 and G3 would have no influence on the live load distribution factor of girder G1 using the lever rule for the bridge cross section shown in Figure 1.

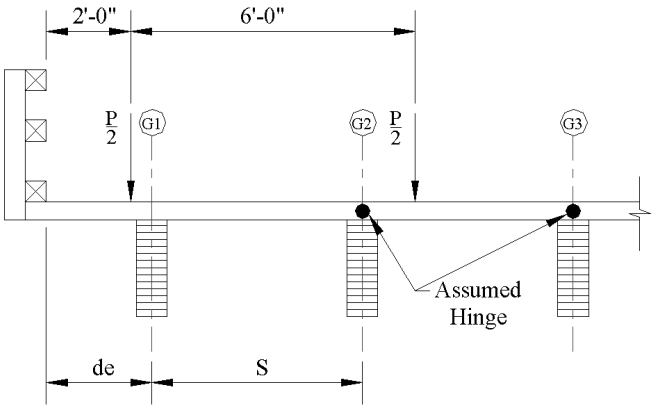

Figure 1. Lever rule distribution Factor

Although the same distribution factor is used for moment and shear, AASHTO does recognize the increase of load near the support with the use of Eq. 1 provided below. This equation is used when investigating shear parallel to the grain and is presented in the 2005 AASHTO LRFD specification 4.6.2.2.2a-1 [2]. This equation is currently based on wheel loads.

$$V_{LL} = 0.5[(0.6V_{LU}) + V_{LD}] \quad (1)$$

Where:

V_{LL} = distribution live load vertical shear (kips)
V_{LU} = maximum vertical shear at 3d or L/4 due to undistributed wheel loads (kips)
V_{LD} = maximum vertical shear at 3d or L/4 due to distributed wheel loads (kips)

Literature Review

In the 1980's the National Cooperative Highway Research Program (NCHRP) Project 12-26, Zokaie T. et.al. [18], began to develop live load distribution equations for girder bridges. The live load distribution equations documented in this report were the basis of the equations that were presented in the 2005 AASHTO LRFD Design Specifications. To develop equations with a wide range of applicability, a large database of bridges with various parameters were selected from randomly selected states. The database consisted of 365 slab-girder bridges, 112 prestressed concrete and 121 reinforced concrete box girder bridges, 67 multi-box beam bridges, 130 slab bridges, and 55 spread box beam bridges [18].

For slab-girder bridges, NCHRP 12-26, Zokaie T. et.al. focused on reinforced concrete T-beams, prestressed concrete I-girders, and steel I-girders. The authors of NCHRP 12-26 developed relationships to calculate live load distribution factors, of the above bridges, for moment and shear. Previously, the AASHTO Standard Specification did not recognize separate distribution factors for moment and shear design. They determined the most significant

parameter to calculate the live load distribution factor to be girder spacing but neglecting the effects of other bridge parameters can result in inaccurate results. These parameters included span length and longitudinal stiffness parameters. Multiple presence factors were included in the distribution factor equations, expect for distribution factors determined by the lever rule where the multiple presence factor is applied as a separate factor. The influence of diaphragms was not included in their research [18].

The current AASHTO LRFD live load distribution equations increased in complexity from the "S/D" AASHTO Standard Specification equations. With the increase in complexity came requests for simplified equations. These requests initiated The National Cooperative Highway Research Program (NCHRP) Project 12-62, conducted by Puckett J. A. et.al. [11]. NCHRP 12-62 created universal, or general, equations capable of representing many bridge types and geometries using simplified methods known in industry. These simplified methods were compared to the calculated analytical live load distribution factors. The uniform, or Henry's Method, and the lever rule were selected based on how well their results correlated to the analytical finite element values. The uniform and lever rule results were calibrated with the affine transformation process and adjusted with the distribution simplification factor [11]. NCHRP Project 12-62, Puckett J. A. et.al. [11] also performed parametric studies on skew angle, diaphragms, and transverse vehicle position with the following conclusions:

- Skew angles less than 30^o had minimal impact on the live load distribution factor results. As the skew angle increased beyond 30^o the live load distribution factor for shear increased while the moment live load distribution factor decreased.
- The diaphragm configuration typically used in practice had minimal influence on the live load distribution factors for moment and shear.

- As the vehicle, or vehicles, were placed further away from the curb, or barrier, the live load distribution factors for moment and shear decreased.
- Barrier stiffness was neglected in the study.

Recent studies (Cai 2005 [5]; Yousif and Hindi 2007 [16]) evaluated the 2005 AASHTO LRFD distribution factor equation for prestressed concrete I-girders. Cai [5] proposed revisions to the stiffness component of the existing live load distribution equation using beam-on-an-elastic foundation theory. Yousif and Hindi [16] analyzed the existing live load distribution equations, recording how the existing LRFD distribution factor and calculated finite element distribution ratio varies with span length. Yousif and Hindi [16] determined that the AASHTO LRFD live load distribution equations, for bridges within the intermediate range of limits specified by AASHTO provided acceptable results. When near the extreme ranges of the AASHTO limitations the results deviated from the finite element results.

In 1994, Gilham and Ritter [8] recognized the need to investigate the "S/D" live load distribution equations for glued laminated timber bridges. Gilham and Ritter [8] studied the distribution of live load in single span longitudinal stringer bridges with transverse timber deck panels. Grillage models were utilized to determine the deflections of 560 bridges under AASHTO single and multiple lane truck loads. With the deflection results, live load distribution factors, for moment, were determined for both interior and exterior stringers. The analytical distribution factors did not compare well to the to the AASHTO "S/D" load distribution values. It was concluded that the AASHTO values did not incorporate all of the parameters which account for the transfer of load. Single and multiple lane load distribution equations were developed for interior and exterior stringers that contain multiple bridge parameters [26].

Several analytical studies have been performed on glued-laminated timber girder at Iowa State University in recent years. Cha [6], and Kurian [9] conducted finite element analyses to investigate the effects of several design parameters on the overall structural behavior of many in-service bridges. The parametric analyses performed by Cha [6] and Kurian [9] examined the effects of boundary conditions and the change in the timber modulus of elasticity. Both Cha [9] and Kurian [6] concluded that the modulus of elasticity has a significant effect on bridge response when comparing the deflections attained from the analytical models to the field data results. Additionally, altering the boundary conditions from simply supported to fixed, of the analytical model, captured the recorded field test displacements. These two studies did not address live load distribution.

Analytical model of glued-laminated timber girder bridges

General

As previously mentioned, several in-service timber bridges were field tested by ISU researchers. The field test data consisted of recorded displacements at, or near, the mid-span of each girder line based on field conditions. This data played an integral role in accomplishing the objectives of this report herein. Live load distribution factors are essentially the percentage, or ratio, of a lane load supported by one girder line. The distribution factors obtained from the field tests were determined using Eq. 2 below [8]. The distribution factors determined from the field tests were used to validate the analytical results. These values were also compared to the 2005 AASHTO LRFD distribution factors.

$$DF_i = \frac{\Delta_i}{\sum_{i=1}^{n} \Delta_i} \; x \; (number \; of \; lanes \; loaded) \qquad (2)$$

Where:

DF_i = lane load distribution factor of the *i*th girder.
D_i = deflection of the *i*th girder.
SD_i = sum of all girder deflections.
n = number of girders.

The 2005 AASHTO LRFD single lane load distribution factor is S/10 for an interior girder, from Table 2. For comparison to the finite element results, the single lane load multiple presence factor of 1.2 from Table 3 was removed from the AASHTO LRFD live load distribution factor. Therefore, a distribution factor value of S/12 was used for interior girders. The lever rule was used to determine the AASHTO LRFD distribution factor for exterior girders. The single lane load multiple presence factor was also excluded from the lever rule live load distribution results plotted for each bridge.

Finite element model of glued-laminated timber girder bridges

The analytical results for this report were obtained with the use of ANSYS [3], a general-purpose finite element program. ANSYS was used to calculate deflections, stresses, and strains that are induced in several in-service bridges under various truck loadings. To facilitate the construction of multiple finite element models, of various timber bridges, it was necessary to develop a preprocessor that simplifies the generation of the models. For this purpose, the ANSYS parametric design language (APDL) was utilized to write the needed preprocessor. To execute the preprocessor the user needs to provide information such as the bridge span length, number of girders, deck thickness, material properties, truckloads, and the boundary conditions. The ANSYS program utilizes the input parameters to generate the finite element model, as shown in Figure 2.

The finite element model panels as well as the girders. The orthotropic timber material in the longitudinal (L), radial (R), and tangential (T) directions of the grain were included. The longitudinal modulus of elasticity is typically known. The orthotropic timber values, related to the longitudinal modulus of elasticity, used for this report herein were provided in the FPL 1999 Wood Handbook [7]. The FPL 1999 Wood Handbook [7] provides the twelve constants required to represent the orthotropic properties of timber. The selected timber species was Douglas-fir, which is a typical softwood species used for glued-laminated timber beams.

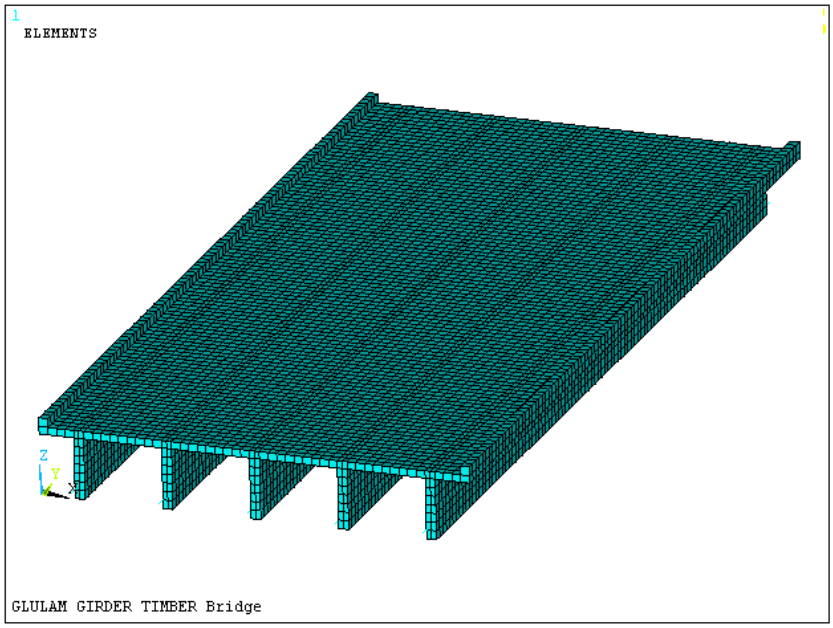

Figure 2. Three dimensional rendering of the finite element model

The finite element models constructed with the preprocessor assume the deck panels and the girders act compositely. The preprocessor allowed the user to model the deck panels as individual deck panels, or as one single deck panel. The later was included in the modeling since the deck panels may act as one single panel due to swelling of the deck panels. The preprocessor allows the user to model the supports of the timber bridges as simply supported with the option of connecting the girder to the backwall, as shown in Figure 3. An as-built example of this

connection detail is illustrated in Figure 4. utilized bilinear solid "brick" elements to model the timber deck.

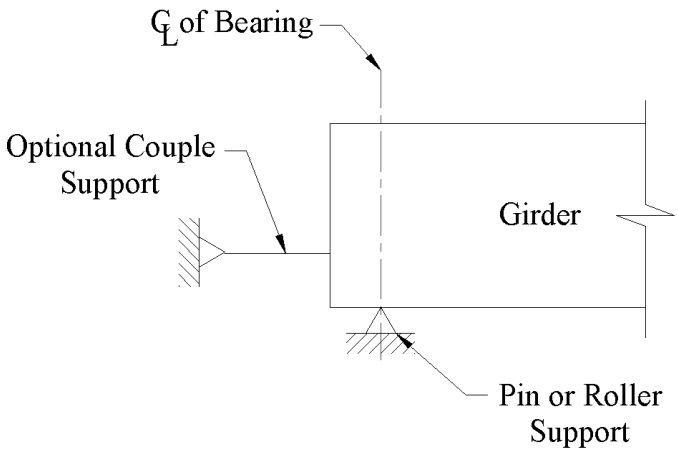

Figure 3. Finite element boundary condition

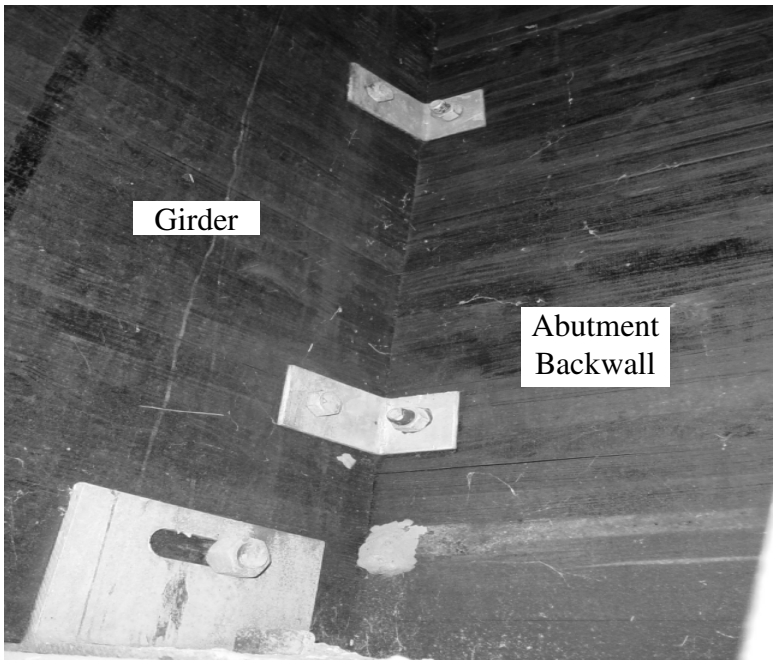

Figure 4. Girder to abutment backwall connection

As previously mentioned, four in-service glued-laminated timber bridges were analyzed using the ANSYS program described previously. The bridges analyzed were Badger Creek

Bridge, Chambers Bridge, Russellville Bridge, and Wittson Bridge. These bridges were analyzed under the truckloads and the loads positions utilized in the field tests. The deflection and live load distribution factor results for these bridges are described below.

Badger Creek Bridge

Badger Creek Bridge is located in Mount Hood National Forest in north central Oregon. Badger Creek Bridge is a 30'-11" single span bridge with a clear width of 14'-1". This bridge consists of four glulam girders spaced at 4'-0" with glued laminated deck panels. The wearing surface consists of timber longitudinal planks [12]. The results associated with the load case that induce the maximum deflections, placing the first wheel load 2'-0" from the face of the curb, as obtained from the field test and the finite element analyses are shown in Figure 5.

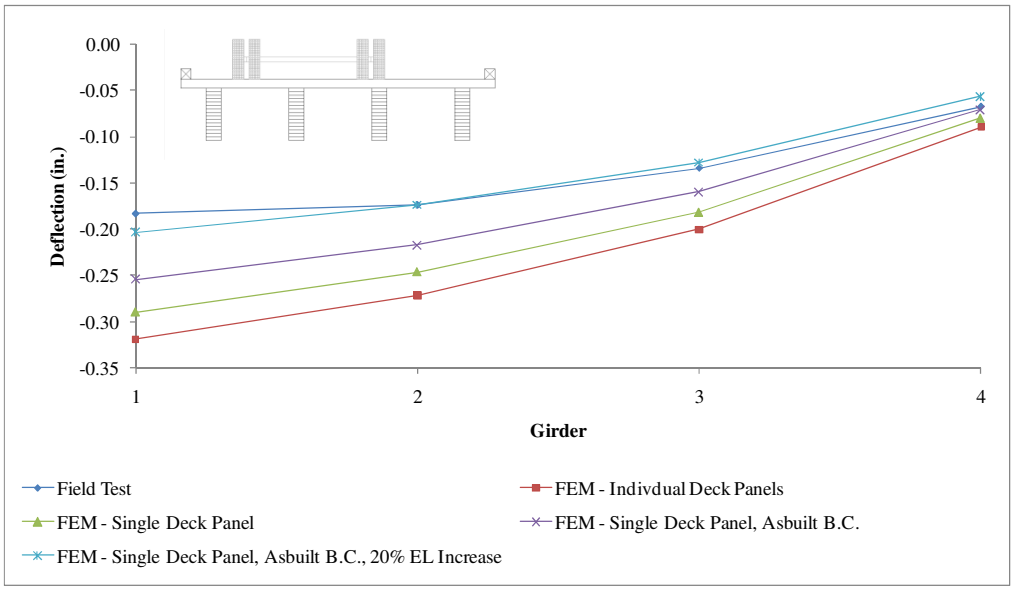

Figure 5. Badger Creek Bridge deflection results

The deflection results from the experimental field test and the finite element analyses are shown above in Figure 5. Notice from Figure 5, modeling the as-built boundary condition and increasing the longitudinal modulus of elasticity of the girders by 20% yielded analytical results that were in good agreement with the field test data. The increase in the modulus of elasticity

was justified due to the uncertainty of the moisture content of the timber.

From Figure 6 below, modifying the boundary condition and modulus of elasticity of the girders had minimal influence to the load distribution results. There is a 10% difference between the finite element and the experimental field test results for girder one. For both the exterior and interior girder, the finite element results were in good agreement with the field test values. There is a 15% difference between the AASHTO LRFD and the field test load distribution results for girder one. The distribution factor results are provided in Table 4.

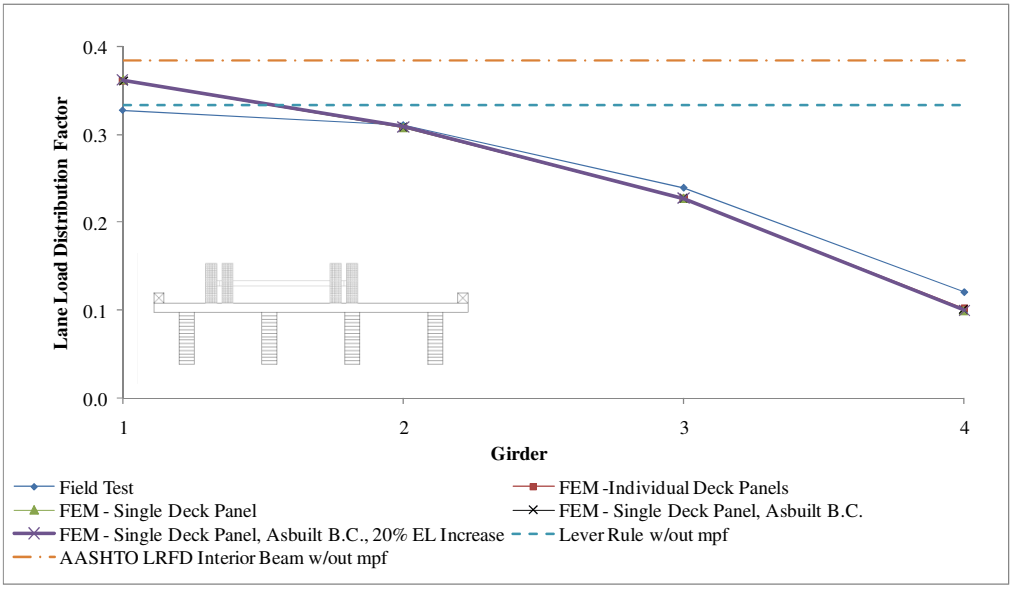

Figure 6. Badger Creek Bridge lane load distribution factors

Table 4. Badger Creek Bridge lane load distribution factors

	Field Test	AASHTO	FEM
Interior Beam	0.311	0.333	0.309
Exterior Beam	0.328	0.385	0.362

As stated previously, modifying the boundary condition and the modulus of elasticity of the girders had minimal influence on the load distribution results shown in Figure 6. Therefore, adjusting for the uncertainty of the modulus of elasticity and the as-built boundary conditions were not included in the analysis of the remaining bridges. In other words, the boundary

conditions for the remaining bridges were modeled as simply supported.

Chambers Bridge

Chambers Bridge is located in east central Alabama. Chambers Bridge is a 51'-6" single span bridge with a clear width of 28'-6". This bridge consists of six glulam girders spaced at 5'-0" with glued laminated deck panels. The wearing surface consists of three inches of asphalt overlay [13]. The results associated with the load case that induce the maximum deflections, placing the first wheel load 2'-3" from the face of the curb, as obtained from the field test and the finite element analyses are shown in Figure 7.

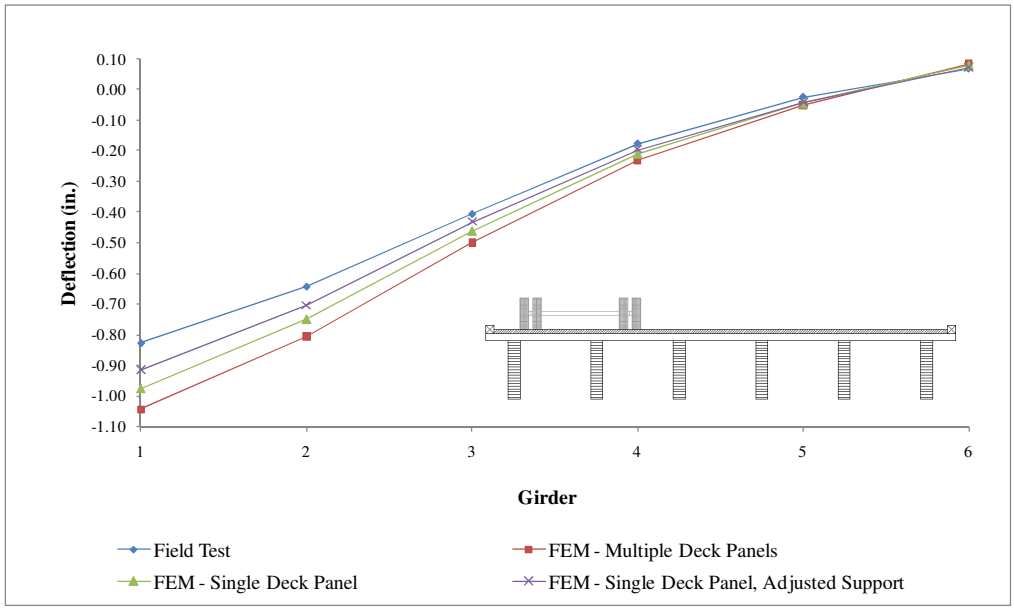

Figure 7. Chambers Bridge deflection results

Notice from Figure 7, modeling the interaction of the deck panels from individual panels to a single panel improves the deflection results. Further modification to the boundary condition and the modulus of elasticity of the girders, similar to Badger Creek, would yield finite element deflection results in good agreement with the field test results.

From Figure 8 below, note the finite element analysis yielded live load distribution results in good agreement to the field test values. There is a 1% difference between the finite element and the experimental field test results for girder one and girder two. The AASHTO LRFD single lane load distribution factors are within a 30% difference of the field test results, controlled by girder two. The distribution factor results are provided in Table 5.

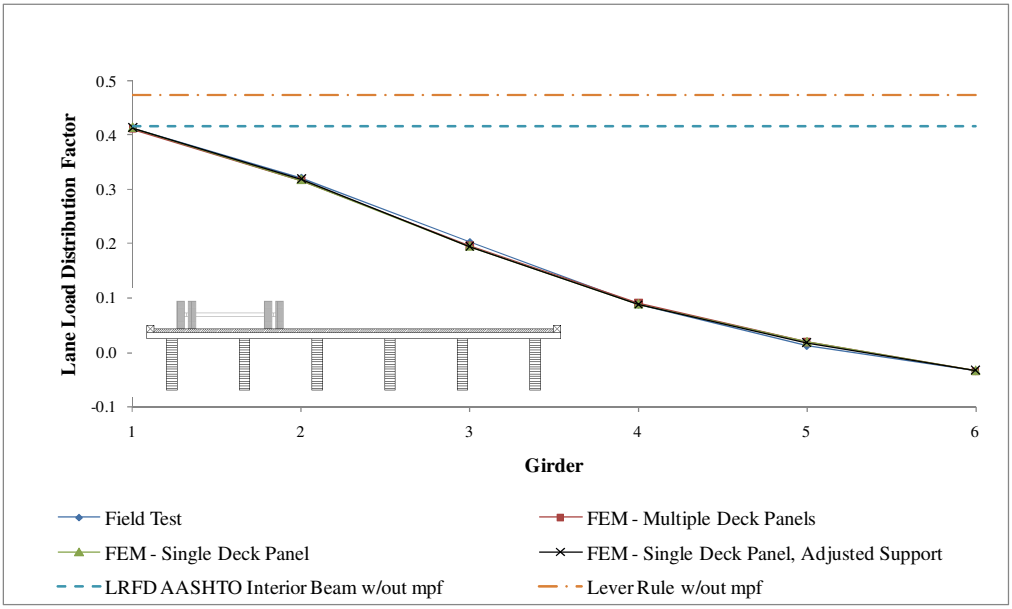

Figure 8. Chambers Bridge lane load distribution factors

Table 5. Chambers Bridge lane load distribution factors

	Field Test	AASHTO	FEM
Interior Beam	0.321	0.417	0.318
Exterior Beam	0.413	0.475	0.414

Russellville Bridge

Russellville Bridge is located in Alabama. Russellville Bridge is a four span bridge, each span is simply supported. One span was field tested. The tested span had a length of 41'-7" with a clear width of 24'-7". This bridge consists of five glulam girders spaced at 5'-0" with glued laminated deck panels. The wearing surface consists of two and half inches of asphalt overlay [14]. The results associated with the load case that induce the maximum deflections, placing the

first wheel load 2'-3" from the face of the curb, as obtained from the field test and the finite element analyses are shown in Figure 9.

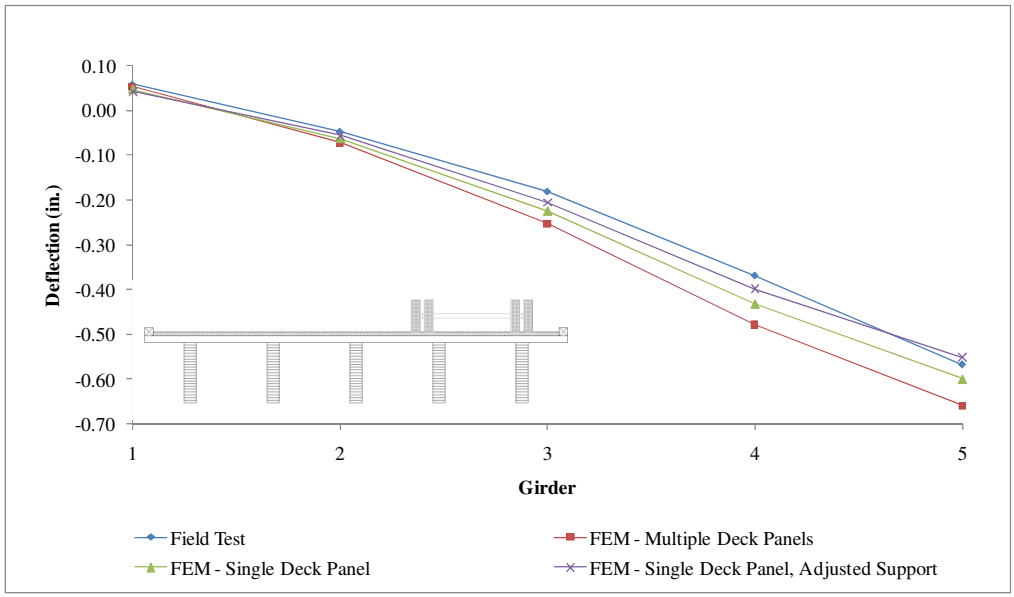

Figure 9. Russellville Bridge deflection results

One can observe from Figure 9 that modifying the interaction of the deck panels from individual panels to a single panel improves the displacement results. Modifying the boundary condition and modulus of elasticity of the girders, similar to Badger Creek, would produce finite element deflection results similar to the field test values.

From Figure 10 below, notice the finite element live load distribution results agree well to the field test values. There is an 8% difference between the finite element and the field test results, controlled by girder five. The AASHTO LRFD single lane load distribution factors are within a 25% difference of the field test results, controlled by girder four. The controlling distribution factor results are provided in Table 6.

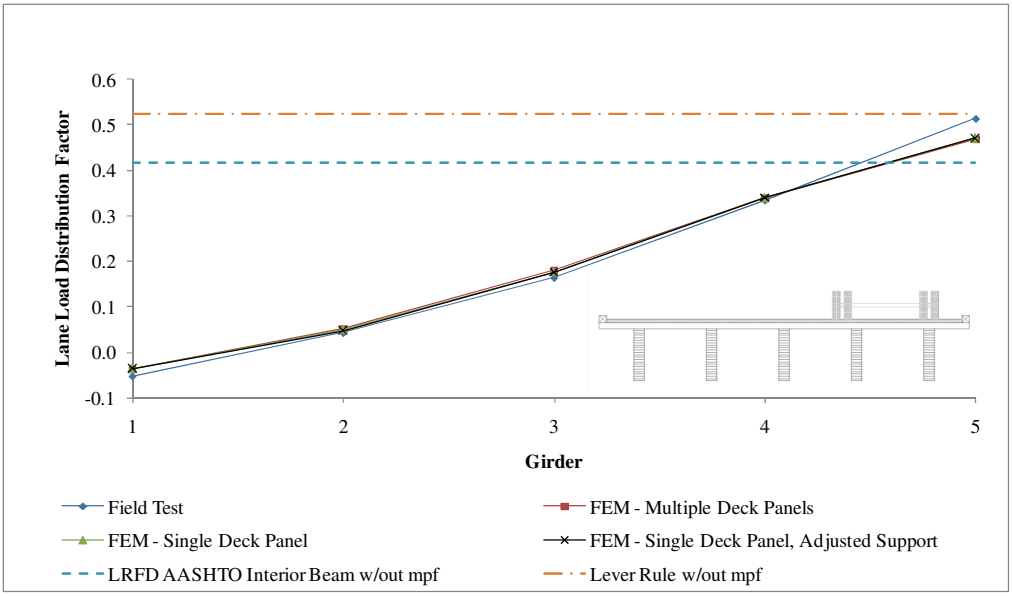

Figure 10. Russellville Bridge lane load distribution factors

Table 6. Russellville Bridge lane load distribution factors

	Field Test	AASHTO	FEM
Interior Beam	0.334	0.417	0.340
Exterior Beam	0.514	0.525	0.471

For Russellville Bridge, a similar load case to the one above was also reviewed. When the field test truck was placed on the opposite side of the bridge at the same distance from the face of the curb, the field test distribution factors of 0.337 for the interior girder and 0.476 for the exterior girder were recorded. These results compare well to the finite element results listed in Table 6.

Wittson Bridge

Wittson Bridge is located in Alabama. Wittson Bridge is a four span bridge and each span is simply supported. One span was field tested. The tested span had a length of 102'-0" with a clear width of 16'-0". This bridge consists of four glulam girders spaced at 4'-3" with glued laminated deck panels. The wearing surface consists of two and half inches of asphalt overlay [15]. The results associated with the load case that induce the maximum deflections as

attained from the field test and the finite element analyses are shown in Figure 11.

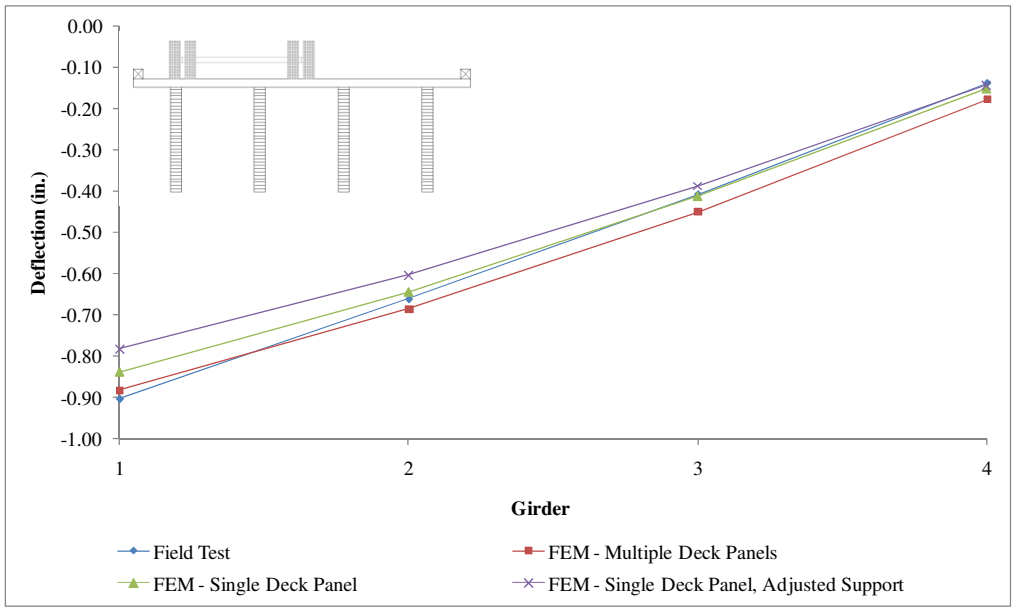

Figure 11. Wittson Bridge deflection results

The deflection results of the field test and finite element analyses are shown above in Figure 11. Notice from Figure 11, modifying the interaction of the deck panels from individual panels to a single panel improves the displacement results. The finite element analyses generated results capturing the field test values.

From Figure 12 below, observe the finite element live load distribution results compare well to the field test values. There is a 5% difference between the finite element and the field test results, controlled by girder one. The AASHTO LRFD single lane load distribution factors are within a 13% difference of the field test values, controlled by girder two. The controlling distribution factor results are provided in Table 8.

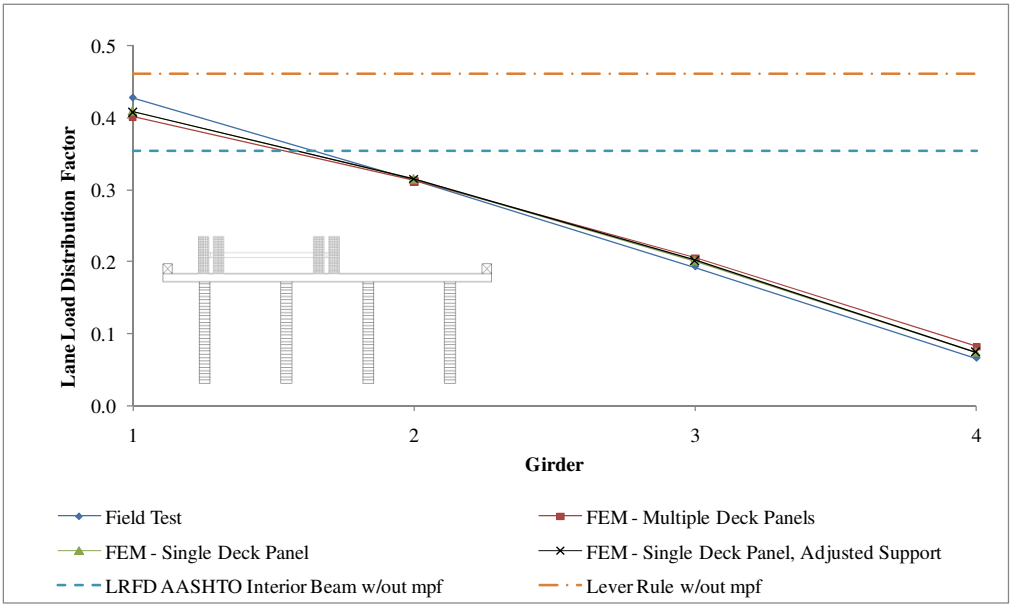

Figure 12. Wittson Bridge lane load distribution factors

Table 7. Wittson Bridge lane load distribution factors

	Field Test	AASHTO	FEM
Interior Beam	0.313	0.354	0.315
Exterior Beam	0.428	0.461	0.408

The influence of load position on the distribution of load

Additional analyses were performed on Chambers Bridge to examine the effects of load position. The above field test analyses focus on the load distribution factors for flexure, or moment only. The additional analyses consisted of using only one truck axle load of 32 kips, or two wheel loads of 16 kips each. One wheel load was place directly above the first exterior girder. The second wheel load was placed six feet away from the previous wheel load, toward the interior of the bridge. Additional axle loads were neglected for simplicity.

The first analysis consisted of determining the load distribution factors placing the axle load at the mid-span of the bridge. The displacement contour plot is shown in Figure 13. Under this load condition, the exterior girder has a load distribution factor of 0.44 and 0.34 for the

interior girder. Increasing the longitudinal modulus of elasticity, of the girder only, by a factor of 1000 increases the lane load distribution factor of the exterior girder to 0.49 and the interior girder to 0.47. The displacement contour plot associated with this load case is shown in Figure 14.

The AASHTO LRFD distribution factor for the exterior girder is 0.50 determined by the lever rule. The lever rule compares well to the 0.49 distribution factor determined after the modulus of elasticity was increased. The discrepancy between the lever rule and finite element analysis values are attributed to the assumptions of the lever rule, which considers the girders to act as infinitely rigid supports and the exclusion of the continuity effects of the deck over the girders.

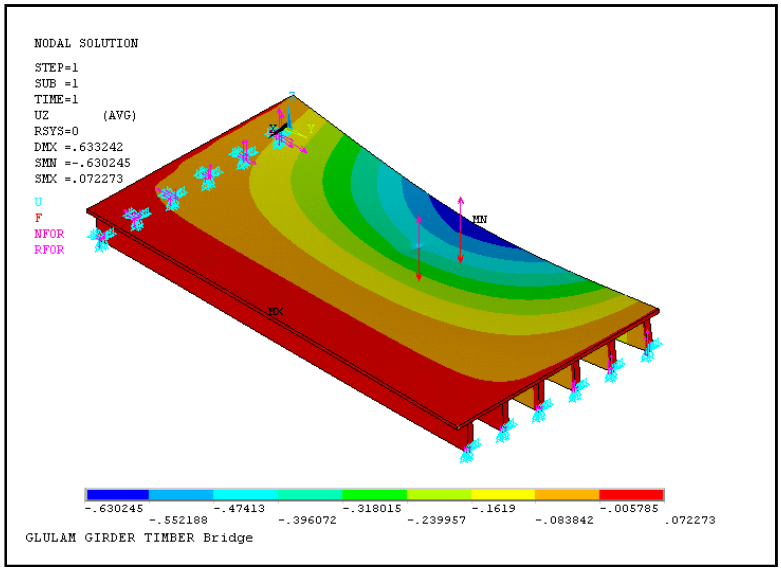

Figure 13. Displacement contour plot

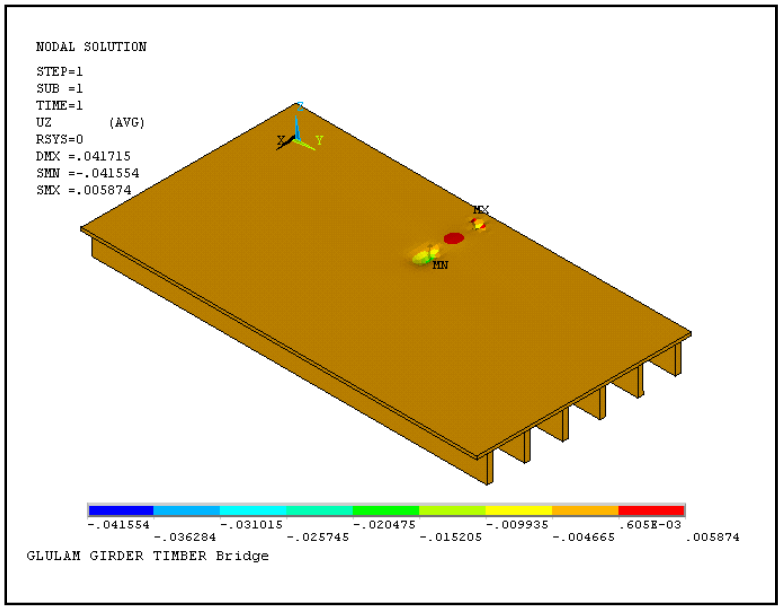

Figure 14. Displacement contour plot ELx1000

The following analysis consisted of adjusting the longitudinal position of the load, from the previous load case, to create the worst-case shear and reaction distribution factors. The controlling distribution factors were determined when the axle load was place near the support. Under this load condition, the exterior girder has a lane load distribution factor of 0.48 and 0.43 for the interior girder. The modulus of elasticity had minimal influence on the reaction distribution factors, as expected. The AASHTO LRFD distribution factor for the exterior girder is 0.50 determined by the lever rule. As stated above, the discrepancy between the lever rule and finite element analysis values is attributed to the assumptions of the lever rule.

The above analyses place one wheel load directly above an exterior girder. Additional trials were examined placing one wheel load directly above an interior girder. The second wheel load was placed six feet away from the previous wheel load, toward the interior of the bridge. The single axle load was placed near the support for the worst-case reaction, three girder depths from the support for shear per AASHTO, and at the mid-span for the worst-case moment

distribution factors. The live load distribution factors, of the interior girder, decrease as the load moves longitudinally from the support towards the mid-span of the bridge, 0.44 to 0.31 respectively. There is a 11% reduction in the load distribution factor when placing the load near the support, 0.44, compared to placing the load three girder depths from the support, 0.39.

Development of live load distribution equations for timber bridges

General

The results summarized above demonstrate that the analytical model produces acceptable live load distribution factors when compared to the results of the field tested in-service bridges. However, the AASHTO load distribution equations tended to yield results that were larger than the field test results. Therefore, the finite element modeling approach previously described was used to analyze a broader range of common glued-laminated timber bridges. This included 32 bridges with varying span lengths, clear widths, and girder spacing. The dimensions for these bridges were selected based on the Standard Plans for Timber Highway Structures [10]. These dimensions are:

- Clear width varied from 12’-0” to 36’-0”.
- Span length varied from 20’-0” to 80’-0”.
- Girder spacing varied from 3’- 4” to 6’- 0”.
- Overhang dimensions, from the face-of-curb to the center of the exterior girder, varied from 12 inches to 30 inches.

In addition, bridges with spans of 100 feet, overhang dimensions that varied from zero to three feet, and various timber moduli of elasticity were also investigated. A total of 102 bridges were analyzed. Of the total bridges, 57 bridges and 45 bridges were used to determine the live

distribution factors for single and multiple truck loadings, respectively.

The truck loading utilized in this work consisted of AASTHO's HL-93 design loads. The AASHTO LRFD design truck (HS20) and design tandem loads were utilized in this study. Additionally, the uniform design lane load affects were neglected. The longitudinal position of the truckload was placed to create either the maximum moment or the maximum shear in the bridge girders. The transverse position of the truck varied from two feet from the face of curb, moving towards the center of the bridge in one foot increments, as shown in Figure 15. A total of ten load cases, five load cases for moment and five load cases for shear, were analyzed for each bridge. The number of load cases were reduced where limited by the clear width of the bridge. For the multiple lane load condition, the second truck was spaced four feet from the truck positions provided in Figure 15.

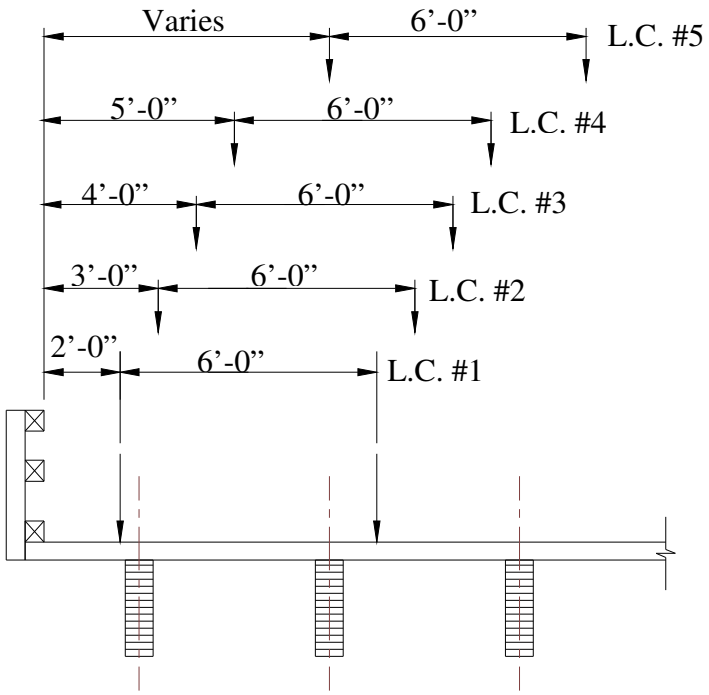

Figure 15. AASHTO HL-93 truck placement

Live load distribution factors were determined from the girder stress results obtained from the finite element models. The finite element results were compared to the current

AASHTO LRFD live load distribution factors for each bridge. Based on the results obtained from the finite element analyses, simplified live load distribution relations were developed for single and multiple design lanes. These live load distribution relations were developed to determine the moment and shear design values for both interior and exterior girders.

Live load moment distribution factors for an interior girder

For each bridge analyzed, the current AASHTO LRFD live load distribution factors (on the vertical axis) were plotted against its respective finite element results (on the horizontal axis). These plots are provided in Figures 16 and 17 for single and multiple lane load conditions, respectively. The multiple presence factors that are associated with the 2005 AASHTO LRFD live load distribution factors were removed from the plotted results below. If the live load distribution factors obtained using the AASHTO LRFD specification correspond similar to the finite element results, one would expect that these results would plot straight line with a slope of unity and would have minimal scatter.

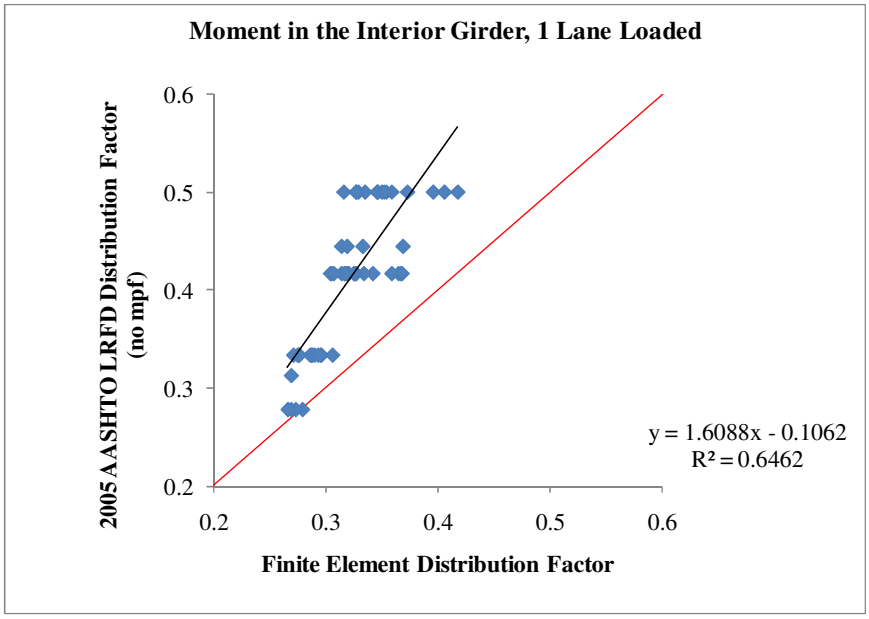

Figure 16. AASHTO LRFD, Moment - Interior Girder, 1 Load Loaded

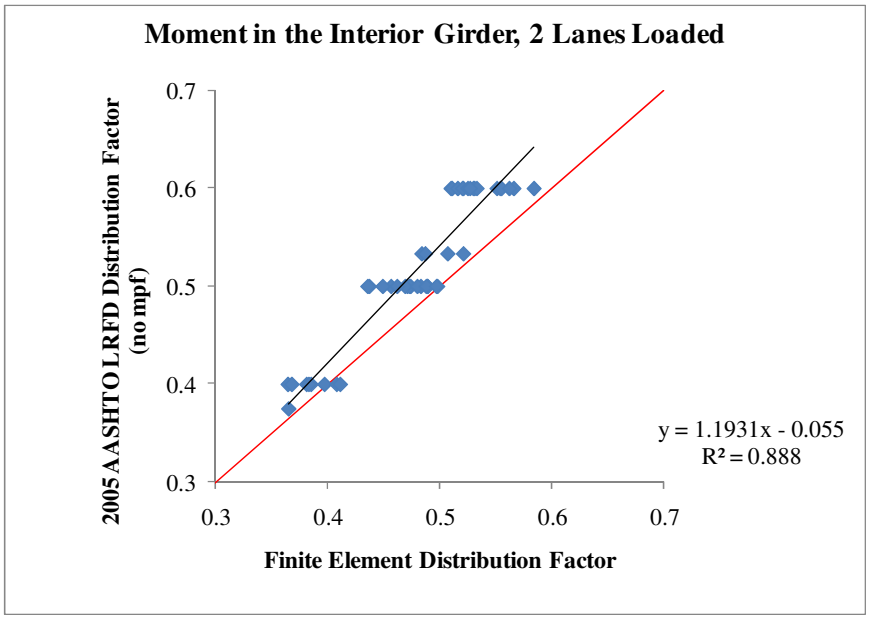

Figure 17. AASHTO LRFD, Moment - Interior Girder 2 Lanes Loaded

As can be observed from the results in Figures 16 and 17, the recommended AASHTO LRFD live load distribution factors overestimate the moment induced in an interior girder under single and multiple lane loadings. On average, the AASHTO LRFD single lane load distribution factors produced results 21% greater than the finite element results. Similar to the single lane load results, the AASHTO LRFD multiple lane load distribution factors yielded a distribution factor that is 7% greater than those obtained from the finite element results.

Other published techniques used for estimating the live load distribution factors, such as the uniform method and the lever rule [11], were also evaluated. For this particular case, the uniform method was explored. The uniform method results, obtained using Eq. 3, were plotted against the finite element results and are provided in Figures 18 and 19 for single and multiple lane loadings, respectively.

$$g_{uniform} = \left(\frac{W_c}{10\ N_g}\right) \quad (3)$$

Where,

$g_{uniform}$ = The uniform method distribution factor

Ng = Number of girders in the bridge cross-section

Wc = Clear roadway width (feet)

From Figures 18 and 19, one can notice the uniform method would yield satisfactory results for determining the live load distribution factor of interior girders under multiple lane loads. On the contrary, the finite element single lane load distribution results did not compare as well to the uniform method. This was expected since the uniform method assumes equal distribution to all girders of the bridge.

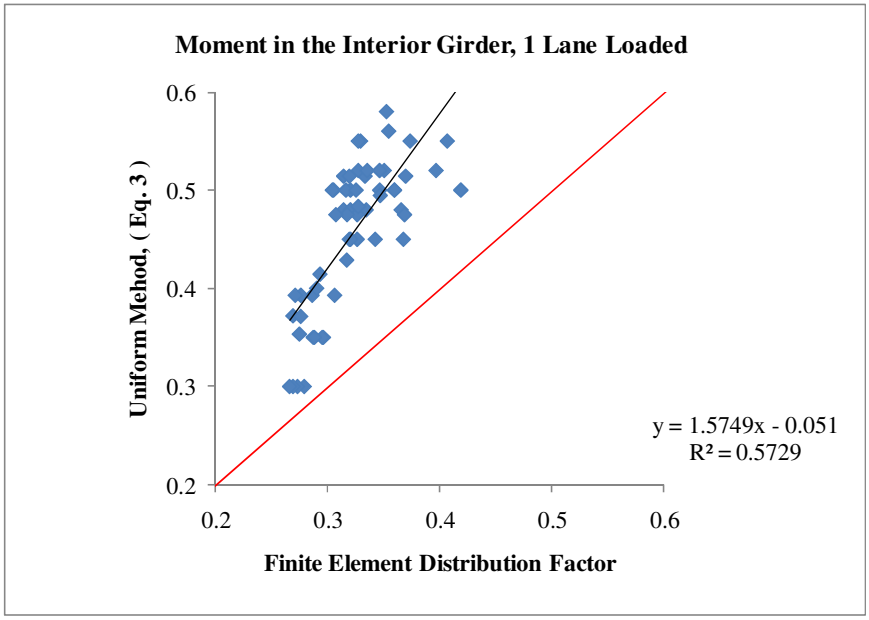

Figure 18. Uniform Method, Moment - Interior Girder 1 Lane Loaded

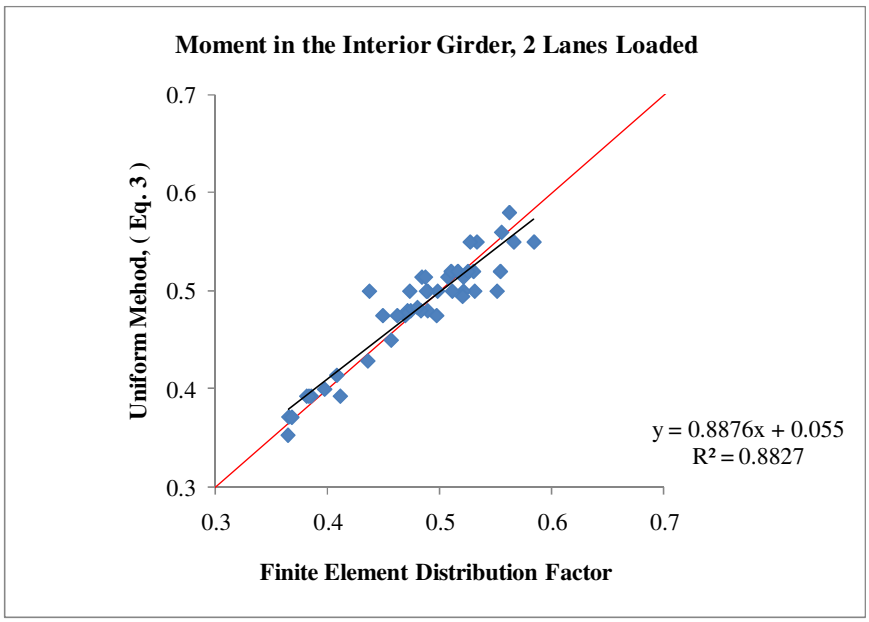

Figure 19. Uniform Method, Moment - Interior Girder 2 Lanes Loaded

Due to the scatter of the uniform method results shown in Figure 18, parametric relations that can be used in determining the live load distribution factors for glued-laminated timber bridges were developed. The parametric equation was developed using the regression analysis solver provided in Microsoft Excel. The same parametric equation can be used for single and multiple lane load conditions. The equation includes variables that are known during the preliminary design phase. The proposed parametric equation is expressed as:

$$g_{pim} = \left(\frac{S}{D}\right)^{exp1} \left(\frac{S}{L}\right)^{exp2} \left(\frac{W_c}{N_g}\right)^{exp3} \quad (4)$$

Where,

D = Constant
exp1 = Constant
exp2 = Constant
exp3 = Constant
g_{pim} = Parametric distribution factor of interior girder
L = Span length, center to center of bearing (feet)
Ng = Number of girders in the bridge cross-section
S = Girder spacing (feet)
Wc = Clear roadway width (feet)

The constant "D" and the three exponents in Eq. 4 were determined by the regression routine, in Microsoft Excel, to produce live load distribution factors, which are correlated to the finite element results. The calculated values for these parameters are listed in Table 8. Eq. 4 was then used in conjunction with the geometry of all of the analyzed bridges to estimate the live load distribution factors. These results were compared with the distribution factors obtained from the finite element analyses, as shown in Figures 20 and 21. Notice from these figures, Eq. 4 produced live load distribution factor results that are very close to those obtained from the finite element analyses. This can be observed from the scatter of the results of Eq. 4 about the solid one-to-one line included in Figures 20 and 21. In other words, one expects the results of Eq. 4 to be equal to the finite element values, i.e. with a linear relation that has a zero intercept and slope of one.

Table 8. Parametric Constants, Moment in the Interior Girder

Loading	D	exp1	exp2	exp3
Single	40	0.409	0.108	-0.018
Multiple	10	0.792	0.058	-0.051

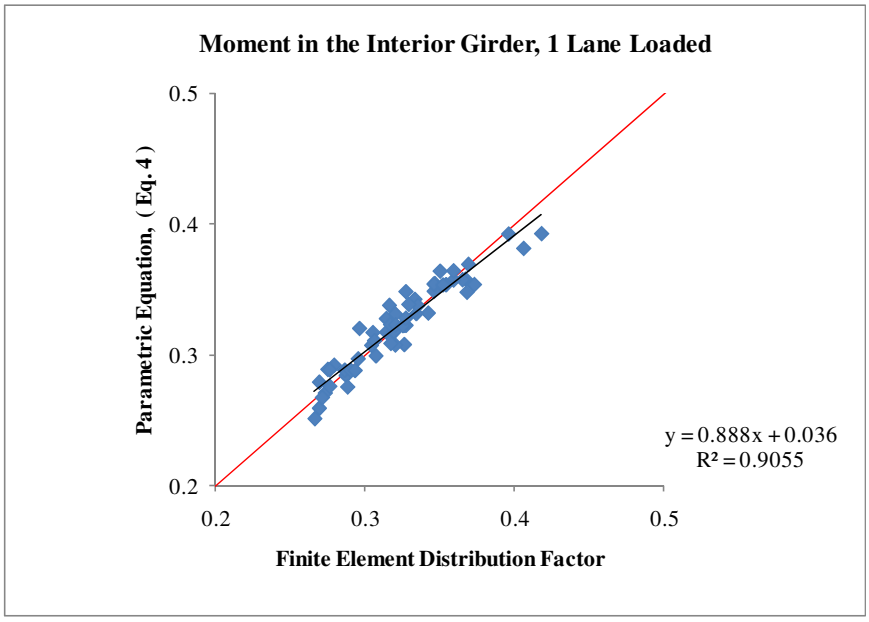

Figure 20. Proposed Parametric Equation, Moment - Interior Girder 1 Lane Loaded

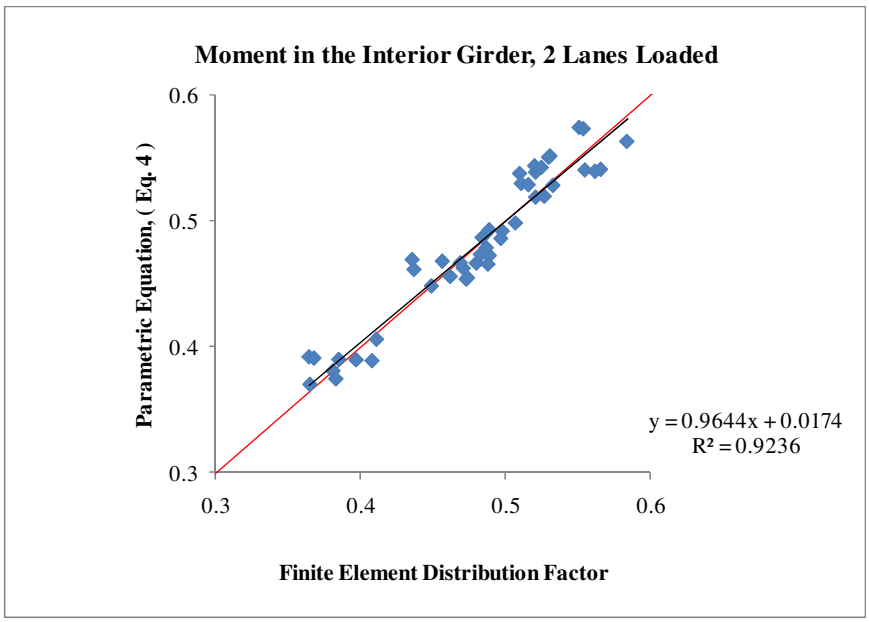

Figure 21. Proposed Parametric Equation, Moment - Interior Girder 2 Lanes Loaded

Using the Excel software, the best-fit line for the ratio of the live load distribution factors obtained using Eq. 4 and the finite element results were determined. For example, Figure 20 yields an equation for the best-fit line as:

$y_1 = 0.888x + 0.036$

Notice that the ratio of Eq. 4 to the finite element results yielded a best-fit line having a slope slightly below one and an intercept slightly above zero. For Eq. 4 to produce a best-fit line that has a slope of one and a zero intercept, when compared to the finite element results, further modification was required. This modification was accomplished utilizing the "affine" transformation process, as summarized by Wolfram Research [17]. The affine transformation process was utilized in NCHRP 12-62 [11]. The "affine" transformation process adjusts the slope and intercept of the best-fit line while preserving collinearity (all points lying on a line will remain on the line after transformation). An example of the affine transformation process is as follows:

The regression best-fit equation from Figure 20 is:

$$y = 0.888x + 0.036$$

Which one can express as:

$$y = a_1x + b_1$$

Where:

a_1 = Slope of the best-fit line
b_1 = Intercept of the best-fit line
x = The finite element live load distribution factor, i.e. the distribution factor one would obtain using finite element analysis.
y = The distribution factor determined from Eq. 4 (g_{pim})

The next step in the affine transformation process is to solve for x in the equation above and substitute y for g_{pim}:

$$x = \frac{g_{pim}}{a_1} - \frac{b_1}{a_1}$$

(x will be referred to as $g_{calibrated}$ from herein)

Let:

$$a = \frac{1}{a_1}$$

$$b = -\frac{b_1}{a_1}$$

Substituting the variables above, the final equation is as follows:

$$g_{calibrated} = \left[a\left(g_{pim}\right) + b\right] \quad (5)$$

To account for any inherent variability of the results obtained from Eq. 5, the distribution simplification factor and the multiple presence factor were next introduced to attain the final live load distribution expression that will be used for design, as shown in Eq. 6. The multiple presence factor in Eq. 6 is kept as a separate term for clarity.

$$mg = \gamma_s m\left[a\left(g_{pim}\right) + b\right] \quad (6)$$

Where:

a = Calibration constant, adjusts trend line slope
b = Calibration constant, adjusts trend line intercept
g_{pim} = Parametric distribution factor, interior girder (Eq. 4)
m = Multiple presence factor
mg = Lane load distribution factor, final adjusted factor
γs = Distribution simplification factor

The distribution simplification factor adjusts the mean results of Eq. 5 to deviate by one-half standard deviation. This is similar to NCHRP 12-62 [11]. An example of the how the distribution simplification factor was determined is provided below:

Using following statistical relationship in Eq. 7:

$$\gamma_s = \left(\frac{1}{\mu_{S/R}}\right) + z_a\left(COV_{S/R}\right) \quad (7)$$

Where:

γs = Distribution simplification factor
$\mu_{S/R}$ = The mean ratio of Eq. 5 and the finite element results
z_a = Number of standard deviations that the method is above the mean of the finite element results, 0.5 was used.
$COV_{S/R}$ = Coefficient of variation

The statistical data provided from Figure 22 produces a distribution simplification factor "γs" of:

$$\gamma_s = \left(\frac{1}{0.999}\right) + 0.5(0.036) = 1.019 \text{ use } 1.02$$

The final live load distribution factors produced by Eq. 6 are shown in Figures 22 and 23 for single and multiple lane loads, respectively. To determine the final live load distribution factors the calibration constants and the distribution simplification factor values in Table 9 were utilized. The multiple presence factors were not included in the plotted results. On average, the

proposed parametric equation produces results 2% greater than the rigorous finite element results due to the distribution simplification factor adjustment.

Table 9. Calibration Constants, Moment in the Interior Girder

Loading	γ_s	a	b	m
Single	1.02	1.126	-0.041	1.2
Multiple	1.02	1.037	-0.018	1

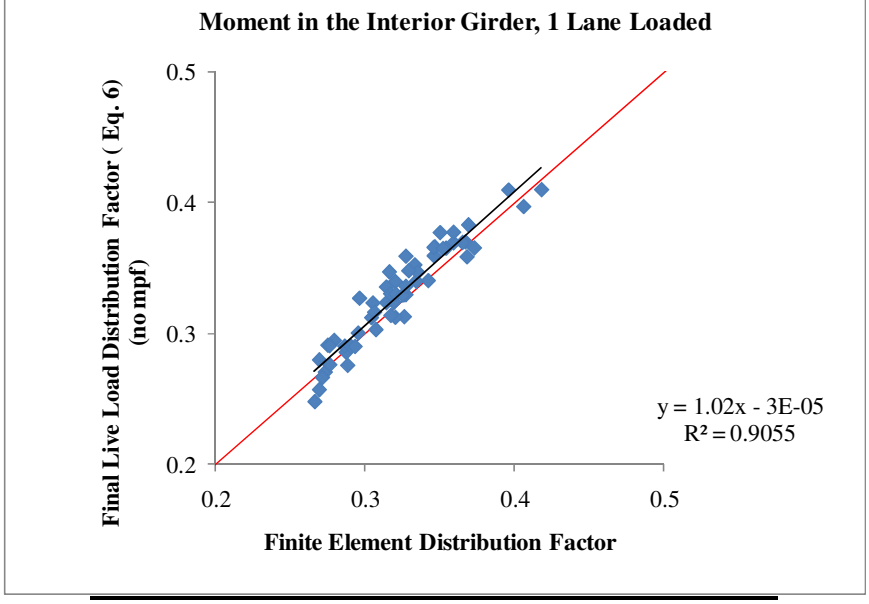

Statisitical Parameters				
γ_S	$\mu_{S/R}$	$COV_{S/R}$	z_a	Count
1.02	0.999	0.036	0.5	57

Figure 22. Final Calibrated Results, Moment - Interior Girder 1 Lane Loaded

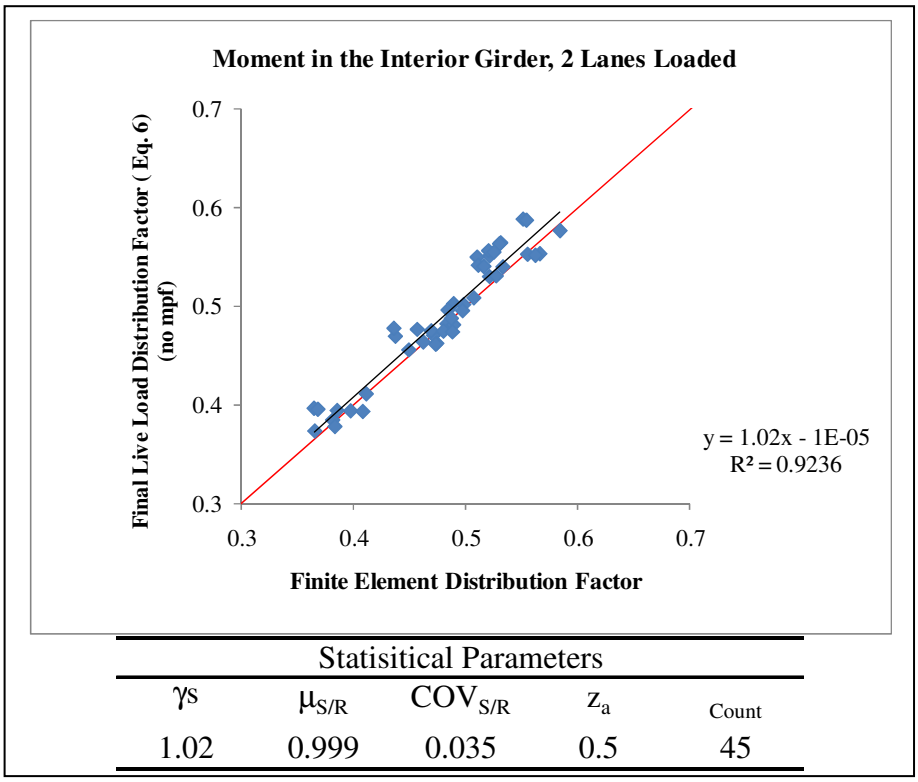

Statisitical Parameters				
γ_S	$\mu_{S/R}$	$COV_{S/R}$	z_a	Count
1.02	0.999	0.035	0.5	45

Figure 23. Final Calibrated Results, Moment - Interior Girder 2 Lanes Loaded

Live load shear distribution factors for an interior girder

The same bridges used above were also analyzed to investigate the live load shear distribution factors for an interior girder. The load was placed to induce the worst-case reaction and shear forces in the bridge girders. These finite element results (in the vertical axis) were plotted against the current 2005 AASHTO LRFD live load distribution results (in the horizontal axis). The single and multiple lane load distribution factor results are plotted in Figures 25 and 26, respectively. The multiple presence factors that are associated with the 2005 AASHTO LRFD live load distribution factors were removed from the plotted results below.

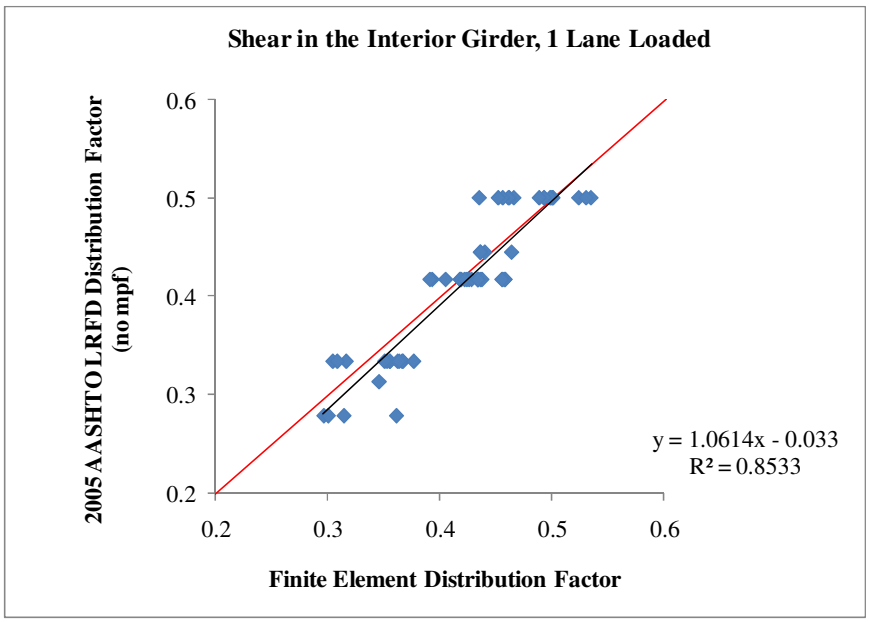

Figure 24. AASHTO LRFD, Shear - Interior Girder 1 Lane Loaded

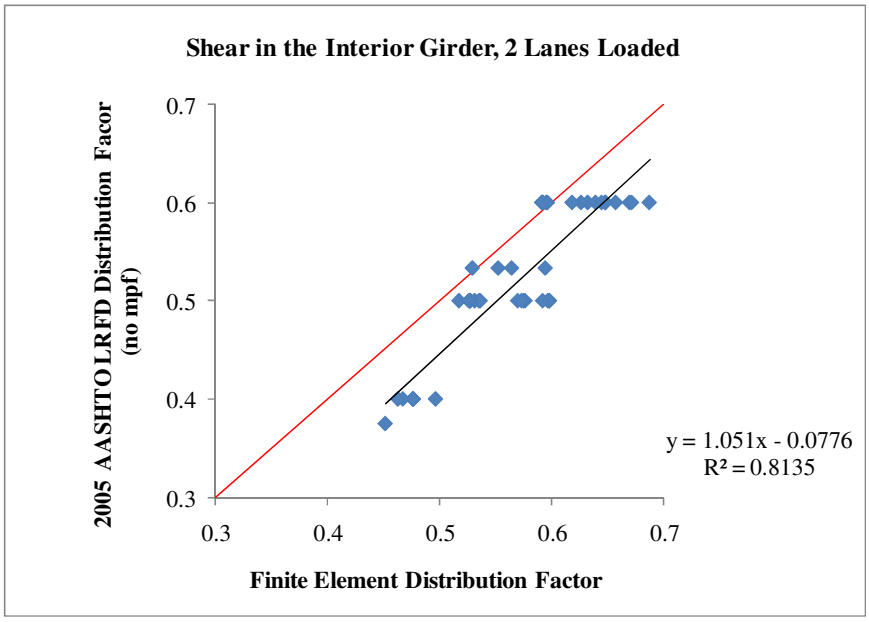

Figure 25. AASHTO LRFD, Shear - Interior Girder 2 Lanes Loaded

Notice from the results in Figures 24 and 25, the recommended AASHTO LRFD live load distribution factors underestimate the shear induced in an interior girder under single and multiple lane loadings. On average, the 2005 AASHTO LRFD distribution factors yielded results 3% less than the finite element results for the single lane load condition. Similar to the

single lane load results, the AASHTO LRFD multiple lane load distribution factors yielded values 10% less than those obtained from the finite element results.

Due to the scatter of the AASHTO LRFD live load distribution results, parametric relations that can be used in determining the live load distributions for glued-laminated timber bridges were developed. The parametric equation was developed using the regression analysis solver provided in Microsoft Excel. The same parametric equation can be used for single and multiple lane load conditions. The equation includes variables that are known during the preliminary design phase. The proposed parametric equation is expressed as:

$$g_{piv} = c\left(\frac{S}{D}\right)^{exp1}\left(\frac{S}{L}\right)^{exp2} \quad (8)$$

Where,

c = Constant
D = Constant
exp1 = Constant
exp2 = Constant
g_{piv} = Parametric distribution factor of interior girder
L = Span length, center to center of bearing (feet)
S = Girder spacing (feet)

The constants in Eq. 8 were determined by the regression routine, in Microsoft Excel, as similarly described above. The calculated values for these parameters are listed in Table 10. Eq. 8 was then used in conjunction with the geometry of all of the analyzed bridges to estimate the live load distribution factors. These results were compared with the distribution factors obtained from the finite element analyses, as shown in Figures 26 and 27. Notice from these figures, Eq. 8 produced live load distribution factor results that are near to those obtained from the finite element analyses. This can be observed from the scatter of the results of Eq. 8 about the solid one-to-one line included in Figures 26 and 27. In other words, one expects the results of Eq. 4 to be equal to the finite element values, i.e. with a linear relation that has a zero intercept and slope

of one.

Table 10. Parametric Constants, Shear in the Interior Girder

Loading	C	D	exp1	exp2
Single	0.92	12	0.719	0.065
Multiple	0.92	10	0.704	-0.015

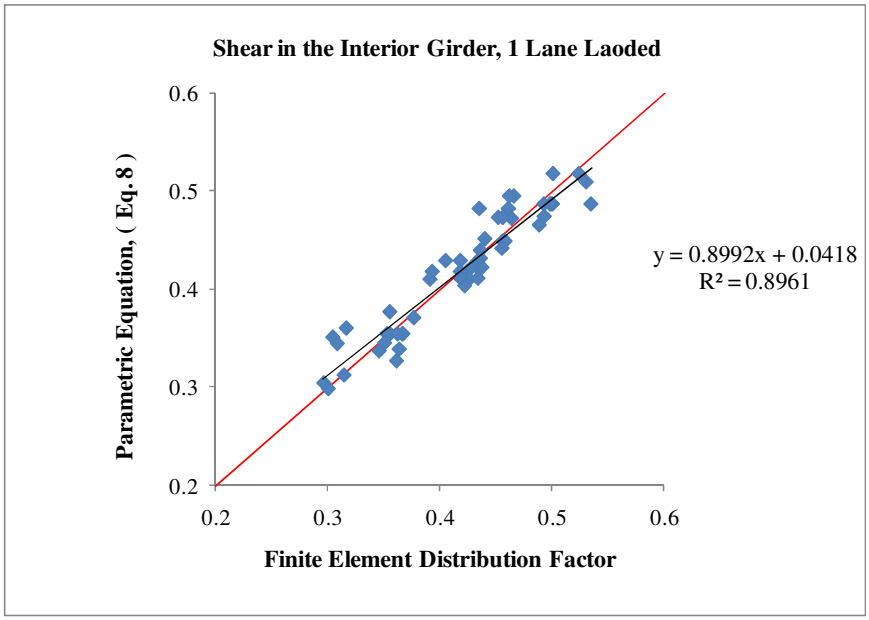

Figure 26. Proposed Equation, Shear - Interior Girder 1 Lane Loaded

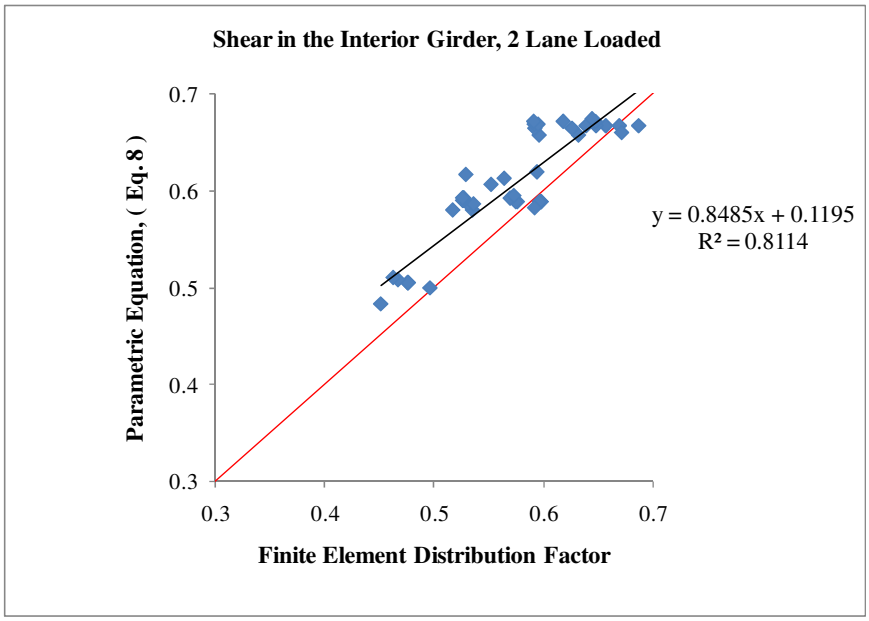

Figure 27. Proposed Equation, Shear - Interior Girder 2 Lanes Loaded

Based on simplification and accuracy, the parametric equation will be used herein to determine the distribution factor for interior girders under single or multiple lane loads. Similar to the approach used in NCHRP 12-62 [11] and as described previously, the final distribution factor used for design will be determined using Eq. 9. To determine the final live load distribution factors, the calibration constants and the distribution simplification factor values in Table 11 were utilized. The final adjusted results are plotted in Figures 28 and 29 for single and multiple lane loads, respectively.

$$mg = \gamma_s m\left[a\left(g_{piv}\right) + b\right] \quad (9)$$

Where:

a = Calibration constant, adjusts trend line slope
b = Calibration constant, adjusts trend line slope intercept
g_{piv} = Parametric distribution factor of interior girder
m = Multiple presence factor
mg = Lane load distribution factor, final adjusted factor
γ_s = Distribution simplification factor

Table 11. Calibration Constants, Shear in the Interior Girder

Loading	γ_s	a	b	m
Single	1.03	1.112	-0.046	1.200
Multiple	1.03	1.179	-0.141	1.000

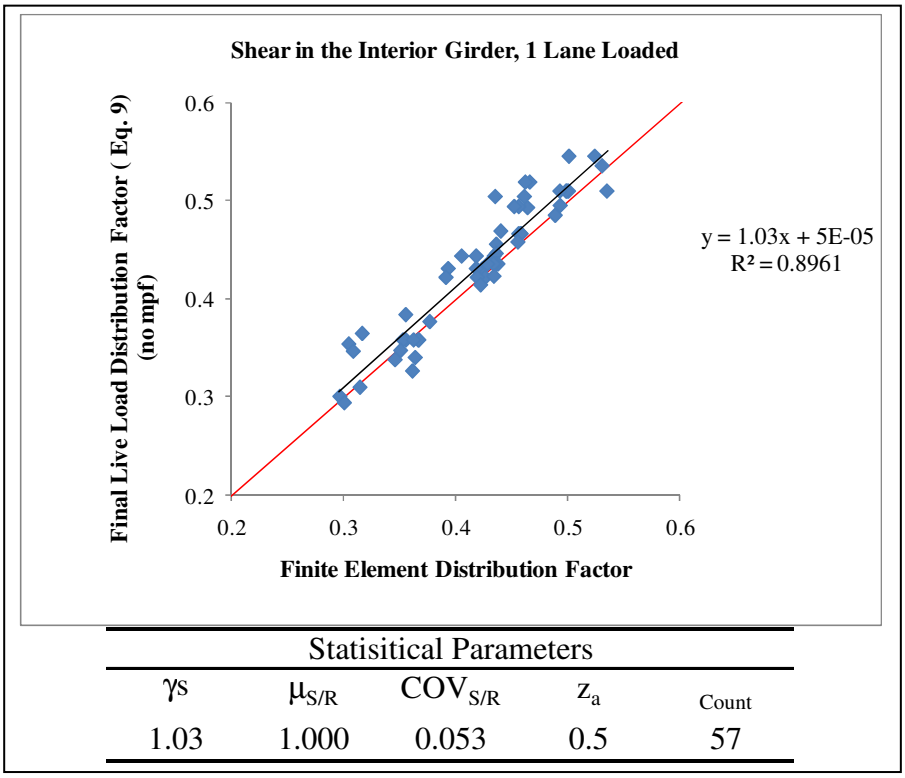

Statisitical Parameters				
γ_S	$\mu_{S/R}$	$COV_{S/R}$	z_a	Count
1.03	1.000	0.053	0.5	57

Figure 28. Final Calibrated Results, Shear - Interior Girder 1 Lane Loaded

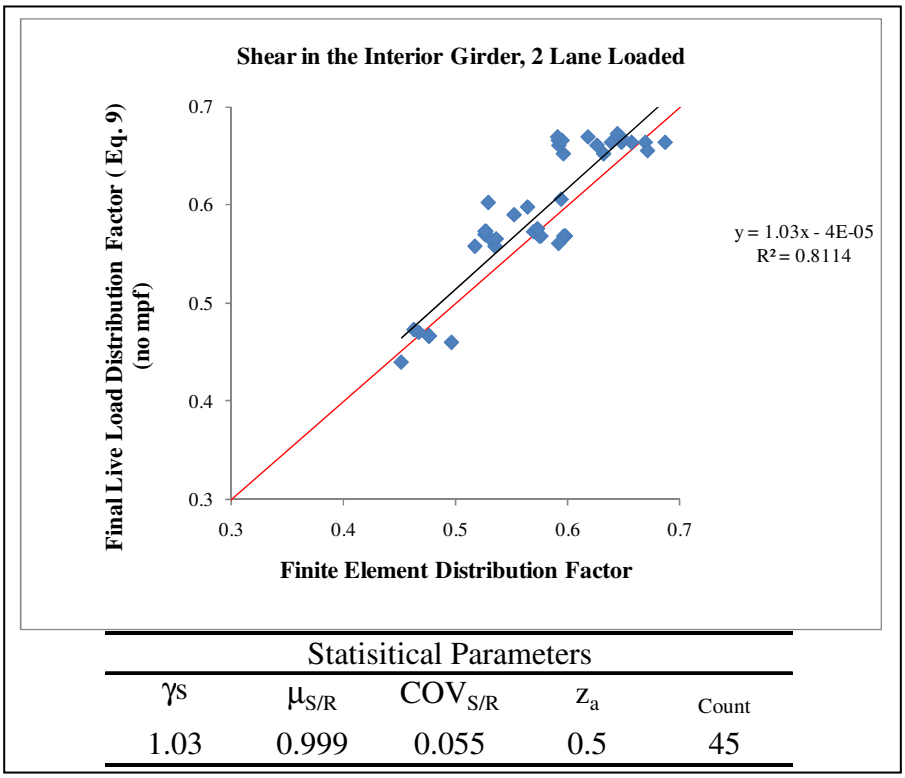

Statisitical Parameters				
γ_S	$\mu_{S/R}$	$COV_{S/R}$	z_a	Count
1.03	0.999	0.055	0.5	45

Figure 29. Final Calibrated Results, Shear - Interior Girder 2 Lanes Loaded

Live load moment distribution factors for an exterior girder

The same bridges used above were analyzed to investigate the live load moment distribution factors for an exterior girder. The load was placed to induce the worst-case moment in the bridge girders. These finite element results (in the vertical axis) were plotted against the current 2005 AASHTO LRFD live load distribution results (in the horizontal axis). Currently, AASHTO utilizes the lever rule to determine the live load moment distribution factor for exterior girders. The single and multiple lane load distribution factor results are plotted in Figures 30 and 31, respectively. The multiple presence factors that are associated with the 2005 AASHTO LRFD live load distribution factors were not included in the plotted results below.

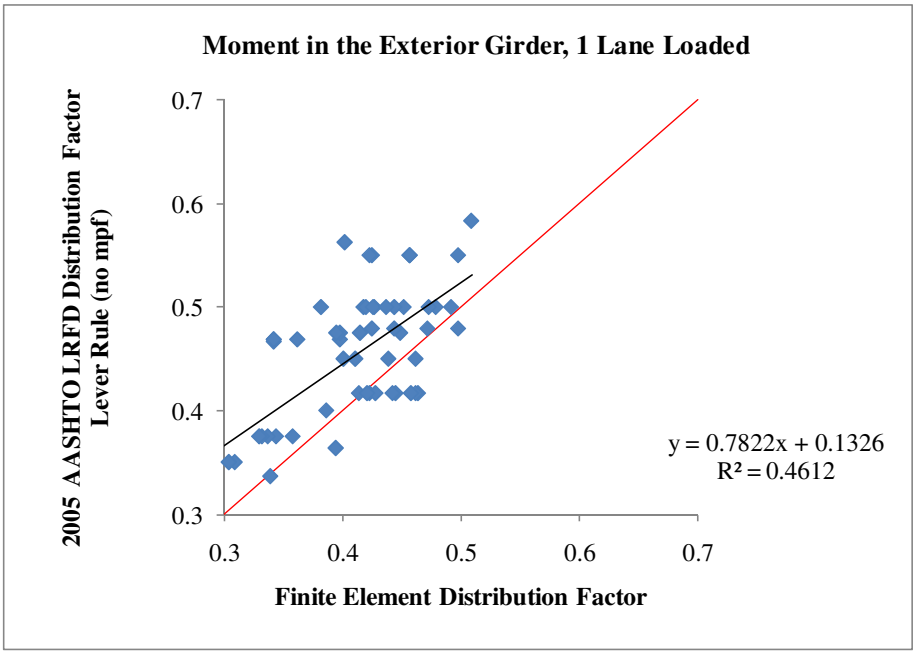

Figure 30. AASHTO LRFD, Moment - Exterior Girder 1 Lane Loaded

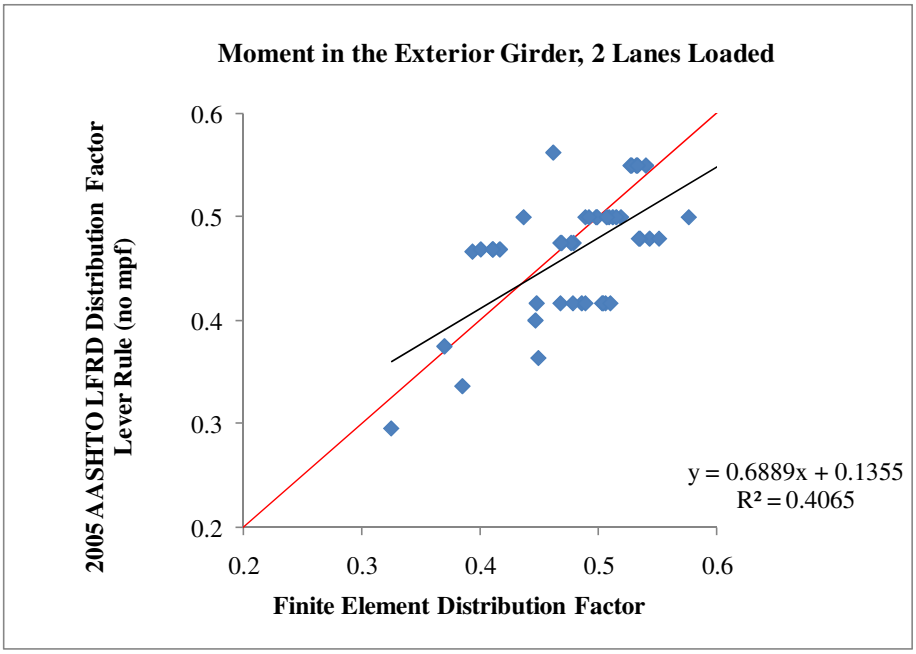

Figure 31. AASHTO LRFD, Moment - Exterior Girder 2 Lanes Loaded

As can be observed from the results in Figures 30 and 31, the recommended AASHTO LRFD live load distribution factors overestimate the moment induced in an exterior girder under single and multiple lane loadings. On average, the AASHTO LRFD single lane load distribution factors produced results 9% greater than the finite element results. Similar to the single lane load results, the AASHTO LRFD multiple lane load distribution factors yielded a distribution factor that is 6% greater than those obtained from the finite element results.

Other published techniques used for estimating the live load distribution factors, such as the uniform method and the lever rule [11], were also evaluated. For this particular case, the uniform method was explored. The uniform method results, obtained using Eq. 3, were plotted against the finite element results and are provided in Figures 32 and 33 for single and multiple lane loadings, respectively.

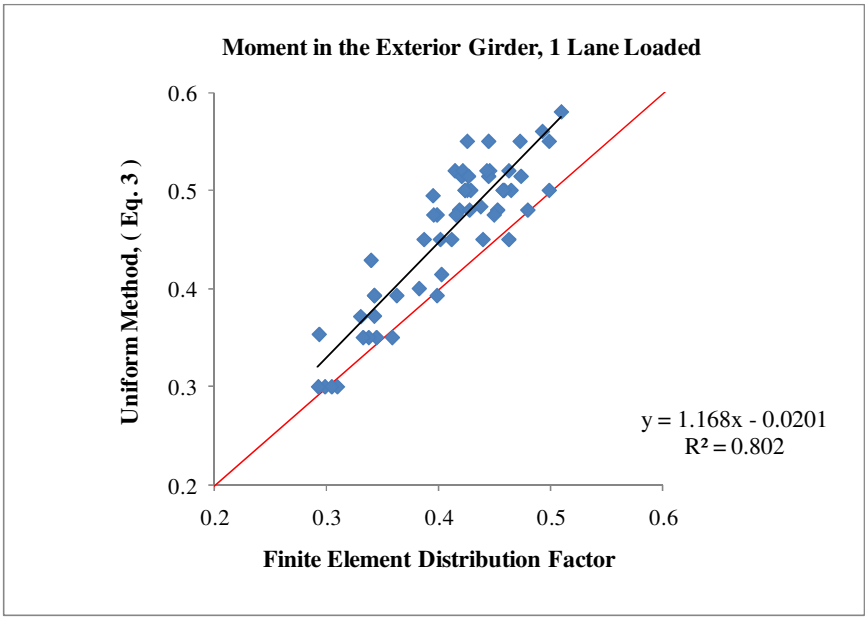

Figure 32. Uniform Method, Moment - Exterior Girder 1 Lane Loaded

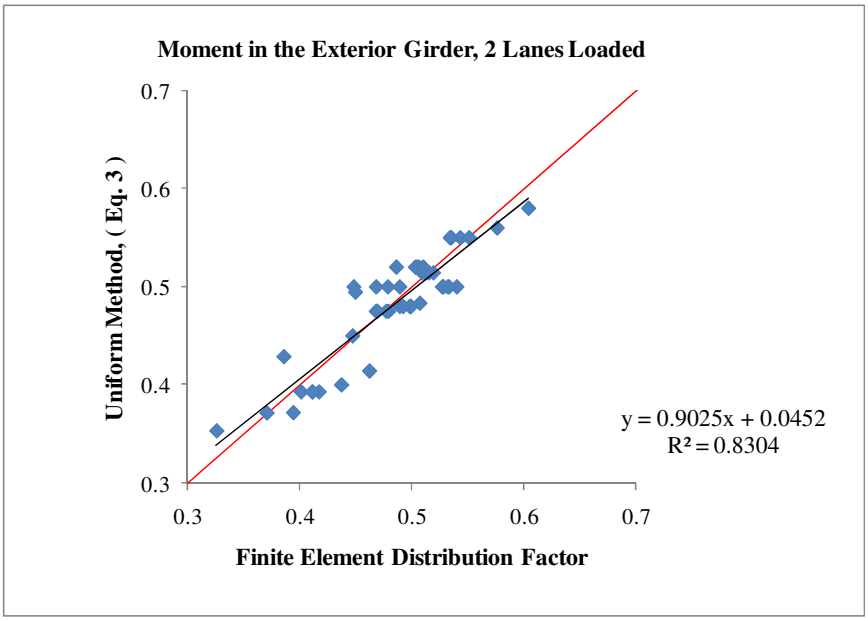

Figure 33. Uniform Method, Moment - Exterior Girder 2 Lanes Loaded

Due to the scatter of the uniform method results shown in Figures 32 and 33, parametric relations that can be used in determining the live load distributions for glued-laminated timber bridges were developed. The parametric equation was developed using the regression analysis solver provided in Microsoft Excel. The same parametric equation can be used for single and

multiple lane load conditions. The equation includes variables that are known during the preliminary design phase. The proposed parametric equation is expressed as:

$$g_{pem} = \left(\frac{S}{D}\right)^{exp1} \left(\frac{S}{L}\right)^{exp2} \left(\frac{d_e}{S}\right)^{exp3} \quad (10)$$

Where,

D = Constant
d_e = Center of exterior girder to face of curb (feet)
exp1 = Constant
exp2 = Constant
exp3 = Constant
g_{pem} = Parametric distribution factor of exterior girder
L = Span length, center to center of bearing (feet)
S = Girder spacing (feet)

The constants in Eq. 10 were determined by the regression routine, in Microsoft Excel, as similarly described above. The calculated values for these parameters are listed in Table 12. Eq. 10 was then used in conjunction with the geometry of all of the analyzed bridges to estimate the live load distribution factors. These results were compared with the distribution factors obtained from the finite element analyses, as shown in Figures 32 and 33. Notice from these figures, Eq. 10 produced live load distribution factor results that are very close to those obtained from the finite element analyses. This can be observed from the scatter of the results of Eq. 10 about the solid one-to-one line included in Figures 34 and 35. In other words, one expects the results of Eq. 10 to be equal to the finite element values, i.e. with a linear relation that has a zero intercept and slope of one.

Table 12. Parametric Constants, Moment in the Exterior Girder

Loading	D	exp1	exp2	exp3
Single	12	0.643	0.075	0.127
Multiple	10	0.821	-0.008	0.166

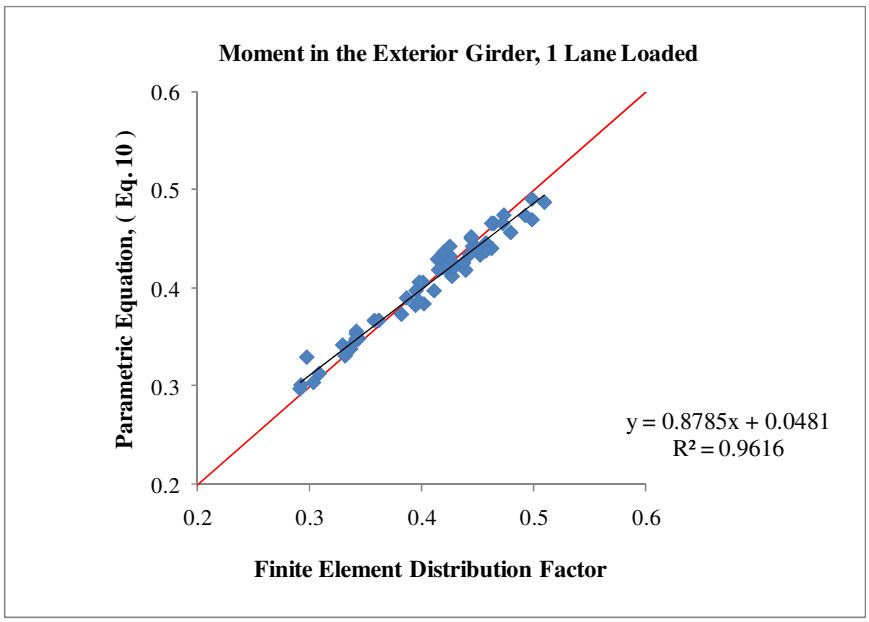

Figure 34. Parametric Equation, Exterior Girder 1 Lane Loaded

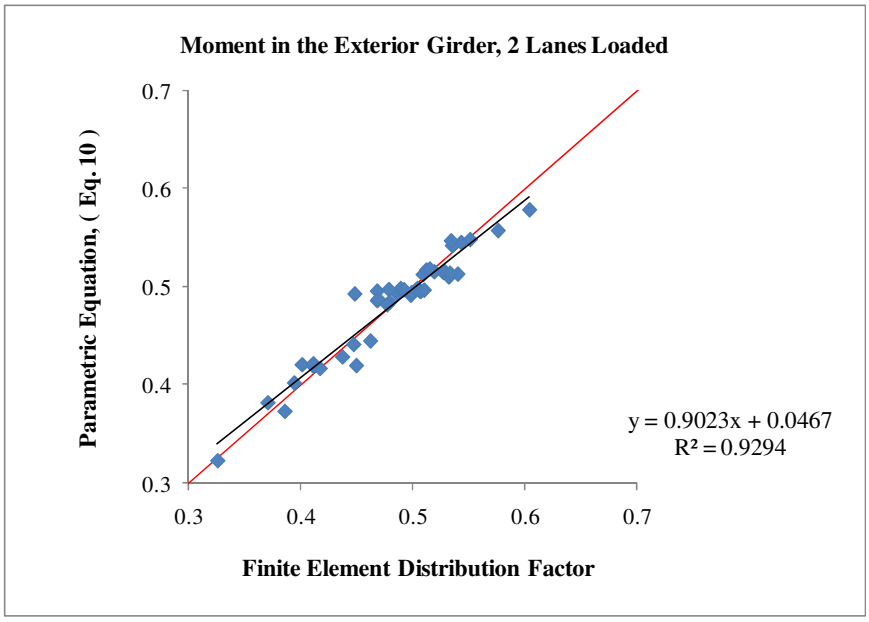

Figure 35. Parametric Equation, Exterior Girder 2 Lanes Loaded

Based on simplification and accuracy, the parametric equation will be used herein to determine the distribution factor for exterior girders under single or multiple lane loads. Similar to the approach used in NCHRP 12-62 [11] and as described previously, the final distribution factor used for design will be determined using Eq. 11. To determine the final live load

distribution factors the calibration constants and the distribution simplification factor values in Table 13 were utilized. The final adjusted results are plotted in Figures 34 and 35 for single and multiple lane loads, respectively.

$$mg = \gamma_s m\left[a\left(g_{pem}\right) + b\right] \quad (11)$$

Where:

a = Calibration constant, adjusts trend line slope
b = Calibration constant, adjusts trend line slope intercept
g_{pem} = Parametric distribution factor of interior girder
m = Multiple presence factor
mg = Lane load distribution factor, final adjusted factor
γs = Distribution simplification factor

Table 13. Calibration Constants, Moment in the Exterior Girder

Loading	γ_s	a	b	m
Single	1.02	1.138	-0.055	1.2
Multiple	1.02	1.108	-0.052	1.0

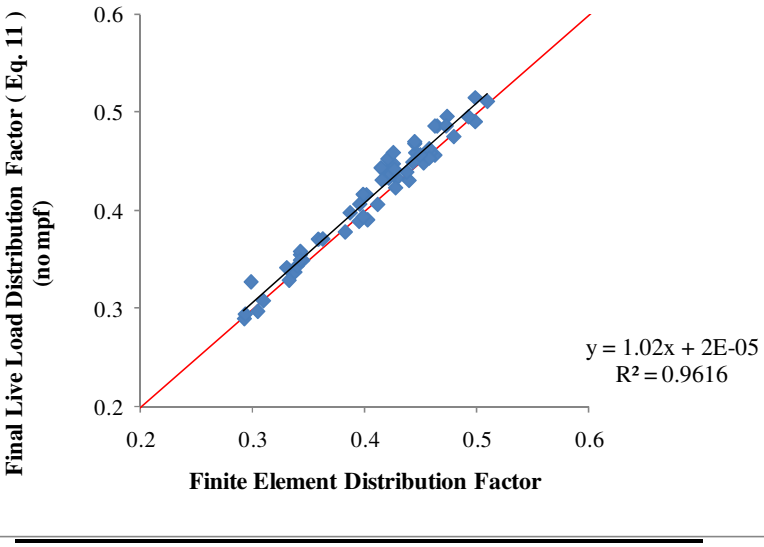

Statisitical Parameters				
γs	$\mu_{S/R}$	$COV_{S/R}$	z_a	Count
1.02	0.999	0.028	0.5	57

Figure 36. Final Calibrated Results, Moment – Exterior Girder 1 Lane Loaded

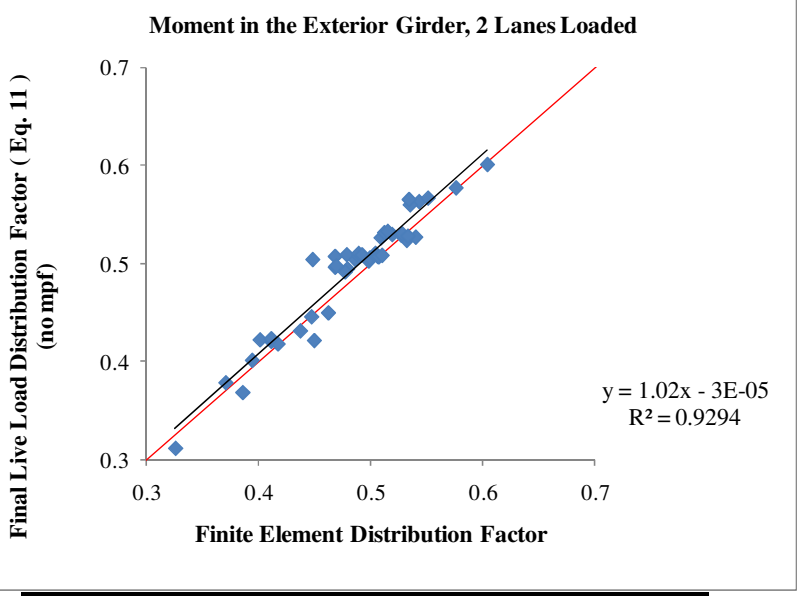

Statisitical Parameters				
γ_S	$\mu_{S/R}$	$COV_{S/R}$	z_a	Count
1.02	0.999	0.034	0.5	45

Figure 37. Final Calibrated Results, Moment – Exterior Girder 2 Lane Loaded

Live load shear distribution factors for an exterior girder

The same bridges used previously were analyzed to investigate the live load shear distribution factors for an exterior girder. The load was placed to induce the worst-case reaction and shear in the bridge girders. These finite element results (in the vertical axis) were plotted against the current 2005 AASHTO LRFD live load distribution results (in the horizontal axis). Currently, AASHTO utilizes the lever rule to determine the live load shear distribution factor for exterior girders. The single and multiple lane load distribution factor results are plotted in Figures 38 and 39, respectively. The multiple presence factors that are associated with the 2005 AASHTO LRFD live load distribution factors were not included in the plotted results below.

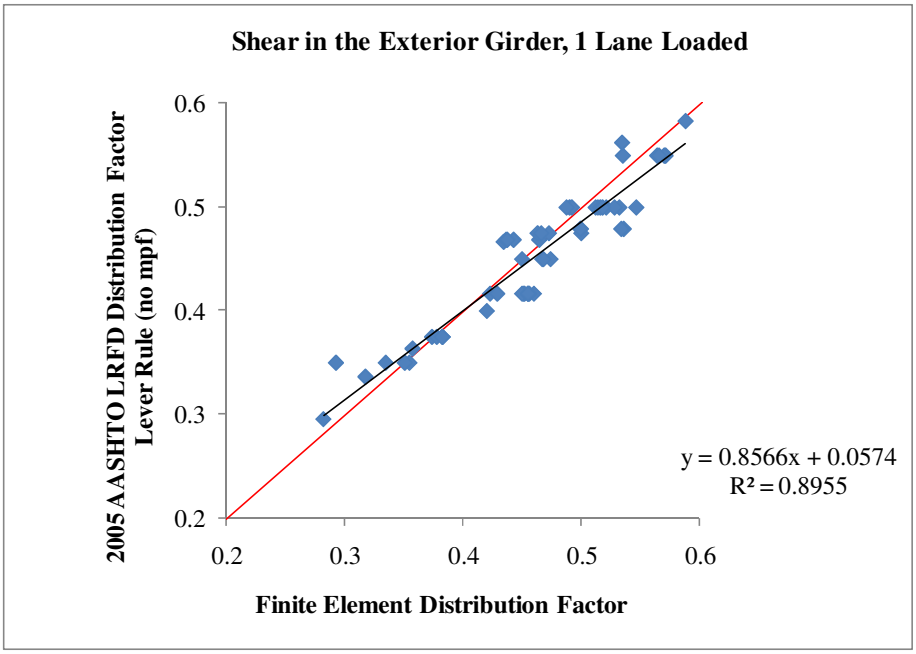

Figure 38. AASHTO LRFD, Shear - Exterior Girder 1 Lane Loaded

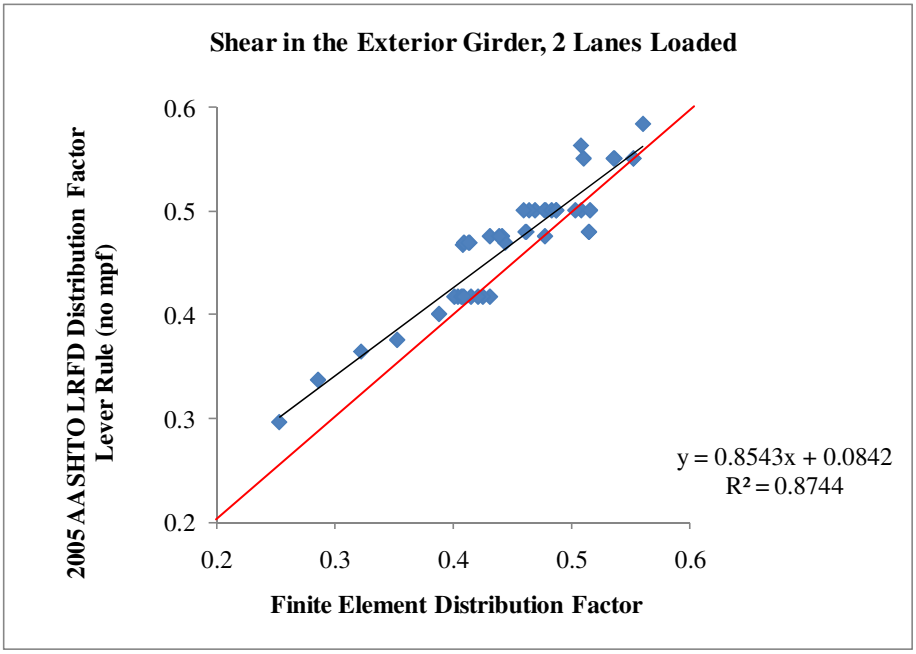

Figure 39. AASHTO LRFD, Shear - Exterior Girder 2 Lanes Loaded

On can notice from the results in Figures 38 and 39, the lever rule produced acceptable results compared to the finite element values. On average, the 2005 AASHTO LRFD distribution factors produced results 2% greater than the finite element results for the single lane

load condition. The multiple lane load AASHTO LRFD distribution factors produced values 7% less than those obtained from the finite element results. The best-fit line equations from both plots have a slope near unity. The correlation (R^2) results from both plots are large, near 0.9. Based on simplicity and accuracy, the lever rule will be used herein to determine the live load shear distribution factors for an exterior girder.

The lever rule distribution factor will be adjusted using the affine transformation process and the distribution simplification factor used in NCHRP 26-62 [11] and as described previously. The final distribution factor used for design is presented in Eq. 12 below. The calibration constants and the distribution simplification factor are provided in Table 14. The final adjusted results are provided in Figures 40 and 41.

$$mg = \gamma_s m[a(g_{lever}) + b] \tag{12}$$

Where:

a = Calibration constant that adjusts trend line slope
b = Calibration constant that adjusts trend line slope intercept
g_{lever} = Lever rule distribution factor of exterior girder
m = Multiple presence factor
mg = Lane load distribution factor, final adjusted factor
γ_s = Distribution simplification factor

Table 14. Calibration Constants, Shear in the Exterior Girder

Loading	γ_s	a	b	m
Single	1.03	1.167	-0.067	1.2
Multiple	1.03	1.171	-0.099	1.0

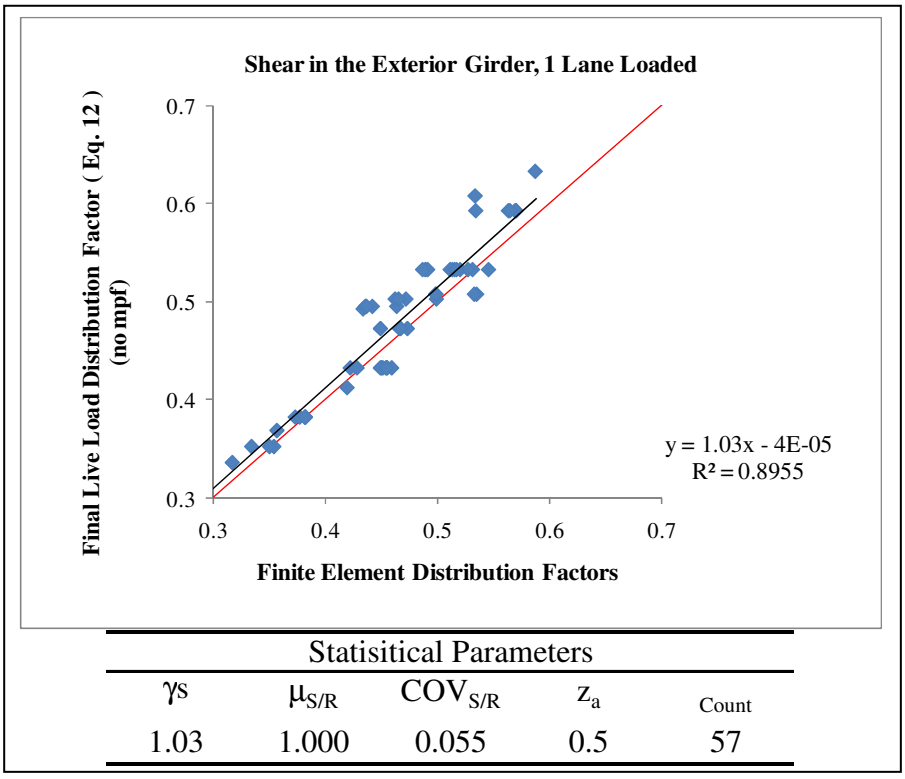

Statisitical Parameters				
γ_S	$\mu_{S/R}$	$COV_{S/R}$	z_a	Count
1.03	1.000	0.055	0.5	57

Figure 40. Final Calibrated Results, Shear – Exterior Girder 1 Lane Loaded

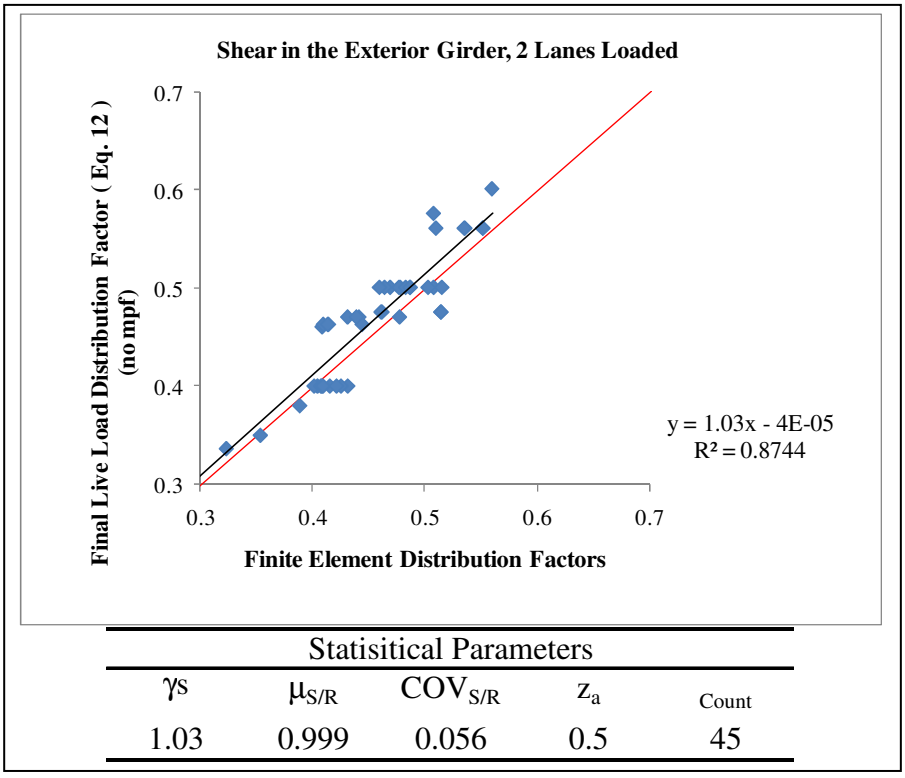

Statisitical Parameters				
γ_S	$\mu_{S/R}$	$COV_{S/R}$	z_a	Count
1.03	0.999	0.056	0.5	45

Figure 41. Final Calibrated Results, Shear – Exterior Girder 2 Lanes Loaded

Summary of the developed live load distribution equations

To replace the existing AASHTO LRFD live load distribution factors, four proposed live load distribution equations with adjustment factors will be presented. The same equation will be used for both single and multiple lane load conditions. Below are the four proposed equations along with the parametric constants, as shown in Table 15, required to compute the live load distribution factors:

Moment in the Interior Girder, 1 and 2 Lanes Loaded

$$g_{pim} = \left(\frac{S}{D}\right)^{exp1}\left(\frac{S}{L}\right)^{exp2}\left(\frac{W_c}{N_g}\right)^{exp3} \quad (4)$$

Shear in the Interior Girder, 1 and 2 Lanes Loaded

$$g_{piv} = c\left(\frac{S}{D}\right)^{exp1}\left(\frac{S}{L}\right)^{exp2} \quad (8)$$

Moment in the Exterior Girder, 1 and 2 Lanes Loaded

$$g_{pem} = \left(\frac{S}{D}\right)^{exp1}\left(\frac{S}{L}\right)^{exp2}\left(\frac{d_e}{S}\right)^{exp3} \quad (10)$$

Shear in the Exterior Girder, 1 and 2 Lanes Loaded

g_{pev} = Lever Rule

Table 15. Parametric constants

	Loading	c	D	exp1	exp2	exp3
Interior	Single	-	40	0.409	0.108	-0.018
Moment	Multiple	-	10	0.792	0.058	-0.051
Interior	Single	0.92	12	0.719	0.065	-
Shear	Multiple	0.92	10	0.704	-0.015	-
Exterior	Single	-	12	0.643	0.075	0.127
Moment	Multiple	-	10	0.821	-0.008	0.166

The live distribution factors determined using the equations above are adjusted using the affine transformation process, distribution simplification factor, and the multiple presence factor. The final live load distribution factors used for design are produced by Eq. 13. The calibration

constants, distribution simplification factor, and the multiple presence factors are provided in Table 16.

$$mg = \gamma_s m\left[a\left(g_{pim}, g_{piv}, g_{pem}, g_{pev}\right) + b\right] \quad (13)$$

Table 16. Calibration constants

	Loading	γ_s	a	b	m
Interior	Single	1.02	1.126	-0.041	1.2
Moment	Multiple	1.02	1.037	-0.018	1
Interior	Single	1.03	1.112	-0.046	1.2
Shear	Multiple	1.03	1.179	-0.141	1
Exterior	Single	1.02	1.138	-0.055	1.2
Moment	Multiple	1.02	1.108	-0.052	1
Exterior	Single	1.03	1.167	-0.067	1.2
Shear	Multiple	1.03	1.171	-0.099	1

Where:

a = Calibration constant, adjusts trend line slope
b = Calibration constant, adjusts trend line slope intercept
c = Constant
D = Constant
d_e = Center of exterior girder to face of curb (feet)
exp1 = Constant
exp2 = Constant
exp3 = Constant
L = Span length, center to center of bearing (feet)
m = Multiple presence factor
mg = Lane load distribution factor, final adjusted factor
Ng = Number of girders in the bridge cross-section
S = Girder spacing (feet)
Wc = Clear roadway width (feet)
γs = Distribution simplification factor

Proposed live load distribution equation example

An example of the proposed equations is provided below for additional clarification. The live load distribution factors from Chamber Bridge, a field tested bridge, will be computed and then compared to the finite element results. Chambers bridge represents a “common” glued-

laminated timber bridge and is within the limits used to develop the proposed live load distribution equations. The multiple presence factors are included in the results below:

Chambers Bridge General Dimensions:
d_e = 1.75 feet
L = 51.5 feet
Ng = 6
S = 5 feet
Wc = 28.5 feet

Moment in the Interior Girder, 1 Lane Loaded Eq. 4

$$g_{pim} = \left(\frac{5}{40}\right)^{0.409}\left(\frac{5}{51.5}\right)^{0.108}\left(\frac{28.5}{6}\right)^{-0.018} = 0.323$$

From Eq. 13

$$mg = 1.02(1.2)[1.126(0.323) - 0.041] = \mathbf{0.394}$$

Moment in the Interior Girder, 2 Lanes Loaded Eq. 4

$$g_{pim} = \left(\frac{5}{10}\right)^{0.792}\left(\frac{5}{51.5}\right)^{0.058}\left(\frac{28.5}{6}\right)^{-0.051} = 0.466$$

From Eq. 13

$$mg = 1.02(1.0)[1.037(0.466) - 0.018] = \mathbf{0.474}$$

Shear in the Interior Girder, 1 Lane Loaded Eq. 8

$$g_{piv} = 0.92\left(\frac{5}{12}\right)^{0.719}\left(\frac{5}{51.5}\right)^{0.065} = 0.421$$

From Eq. 13

$$mg = 1.03(1.2)[1.112(0.421) - 0.046] = \mathbf{0.521}$$

Shear in the Interior Girder, 2 Lanes Loaded Eq. 8

$$g_{piv} = 0.92\left(\frac{5}{10}\right)^{0.704}\left(\frac{5}{51.5}\right)^{-0.015} = 0.585$$

From Eq. 13

$$mg = 1.03(1.0)[1.179(0.585) - 0.141] = \mathbf{0.565}$$

The interior beam live load distribution factors have been summarized in Table 17 below. The proposed equation results compare well to the finite element results. A maximum two percent difference is observed between the finite element and the proposed equation results.

Table 17. Interior beam results summary

Load Condition		FEM	Proposed Equation	AASHTO LRFD
Moment	Single	0.391	0.394	0.5
	Multiple	0.469	0.474	0.5
Shear	Single	0.523	0.521	0.5
	Multiple	0.576	0.565	0.5

Moment in the Exterior Girder, 1 Lane Loaded Eq. 10

$$g_{pem} = \left(\frac{5}{12}\right)^{0.643}\left(\frac{5}{51.5}\right)^{0.075}\left(\frac{1.75}{5}\right)^{0.127} = 0.418$$

From Eq. 13

$$mg = 1.02(1.2)[1.138(0.418) - 0.055] = \mathbf{0.514}$$

Moment in the Exterior Girder, 2 Lanes Loaded Eq. 10

$$g_{pem} = \left(\frac{5}{10}\right)^{0.821}\left(\frac{5}{51.5}\right)^{-0.008}\left(\frac{1.75}{5}\right)^{0.166} = 0.484$$

From Eq. 13

$$mg = 1.02(1.0)[1.108(0.484) - 0.052] = \mathbf{0.493}$$

Shear in the Exterior Girder, 1 Lane Loaded

$$g_{pev} = 0.475 \qquad \text{(from lever rule)}$$

From Eq. 13

$$mg = 1.03(1.2)[1.167(0.475) - 0.067] = \mathbf{0.602}$$

Shear in the Exterior Girder, 2 Lanes Loaded

$$g_{pev} = 0.475 \qquad \text{(from lever rule)}$$

From Eq. 13

$$mg = 1.03(1.0)[1.171(0.475) - 0.099] = \mathbf{0.471}$$

The exterior beam live load distribution factors have been summarized in Table 18 below. The proposed equation results compare well to the finite element results. A maximum seven percent difference is observed between the finite element results and the proposed equation results.

Table 18. Exterior beam results summary

Load Condition		FEM	Proposed Equation	AASHTO LRFD
Moment	Single	0.498	0.514	0.57
	Multiple	0.479	0.493	0.475
Shear	Single	0.568	0.602	0.57
	Multiple	0.441	0.448	0.475

Proposed equation comparison to the field test bridges

The four field tested bridges were used to validate the proposed load distribution equations above. The single lane load moment distribution factors, for interior and exterior girders, were calculated using the proposed equations and compared to the field test results. The multiple presence factors were not included in the results. The finite element distribution factors were determined with stress results due to an HL-93 AASHTO truck load. As stated previously, the field test distribution factors were determined with deflection results. The results for the following bridges are provided below**;** Badger Creek Bridge, Table 18; Chambers Bridge, Table 19; Russellville Bridge, Table 20; and Wittson Bridge, Table 21.

Table 19. Badger Creek Bridge proposed equation results

Girder	Field Test	Proposed	FEM	AASHTO
Interior	0.311	0.310	0.309	0.333
Exterior	0.328	0.357	0.356	0.385

Table 20. Chambers Bridge proposed equation results

Girder	Field Test	Proposed	FEM	AASHTO
Interior	0.321	0.329	0.326	0.417
Exterior	0.413	0.430	0.415	0.475

Table 21. Russellville Bridge proposed equation results

Girder	Field Test	Proposed	FEM	AASHTO
Interior	0.334	0.337	0.335	0.417
Exterior	0.514	0.455	0.477	0.525

Table 22. Wittson Bridge proposed equation results

Girder	Field Test	Proposed	FEM	AASHTO
Interior	0.313	0.276	0.302	0.354
Exterior	0.428	0.359	0.372	0.461

The proposed live load distribution equations produced results within 5% of the finite element results for Badger, Chambers and Russellville Bridge as expected. The proposed exterior girder equation results for Badger Bridge are 9% greater than the field test results. There is a 13% difference between the proposed factor and the field test results of the Russellville exterior girder. The field test results for a similar Russellville load case produced live load distribution factors of 0.337 for the interior girder and 0.476 for the exterior girder. Comparing these results to the proposed equation values, the proposed equation is within a 5% difference. Based on these results, one can conclude that the proposed equation results compare well to both the field test and finite element distribution results.

The Wittson Bridge field test distribution factors are greater than the results from the proposed equation, as listed in Table 21. Wittson Bridge has a span length of 102 feet, which is at the limit of the span length range used in the parametric bridges used to create the proposed equations. It should be recommended that for bridges outside of the parametric bridge range no modifications should be made to the multiple presence factors.

Conclusions

This research involved the evaluation of the existing live load distribution equations for glued-laminated timber girder bridges provided in the 2005 AASHTO LRFD Bridge Design Specification. This was accomplished by using analytical finite element models, which were validated with field data from in-service bridges. The field data consisted of deflections and live

load distribution factors from four glued-laminated timber girder bridges. The validated finite element models were used to perform parametric studies on a broader range of bridges to determine the controlling live load distribution factors. From these parametric bridges, proposed distribution equations were developed.

Minimal changes were made to the glued-laminated timber bridge live load distribution equations from the AASHTO Standard Specification [1] to the 2005 AASHTO LRFD Specification [2]. The changes that did occur to the equations consisted of the conversion from wheel to lane load distribution factors and incorporating the changes to the multiple presence factors. The lever rule method, for exterior girders, remained unchanged. Unlike other bridge types, glued-laminated timber girder bridges do not have separate live load distribution factors for shear. The shear design forces are adjusted with Eq. 1.

Analytical finite element models were developed utilizing ANSYS [3], a general purpose finite element program. The finite element model utilized bilinear solid "brick" elements to model the timber deck panels as well as the girders. The finite element model allowed the user to model the as-built boundary conditions of the field tested bridges. Using the ANSYS parametric design language (APDL) greatly simplified the user input, reducing the modeling time required by the user.

The analytical finite element models were validated with experimental field test results. The analytical deflections and live load distribution values were within an acceptable tolerance to the field test results. Adjusting the deck panel interaction and boundary conditions had minimal influence on the analytical live load distribution factors. Both the analytical and field test results demonstrated that the controlling single lane load moment live load distribution factors occurred when placing the truckload 2'-0" from the face of the curb. This was observed

for both the exterior and interior girders. As the load moves towards the center of the bridge, the load distribution factor in the exterior and interior girders reduces.

A total of 102 bridges were analyzed with the finite element model described above. Of the total bridges, 57 bridges and 45 bridges were used to determine the controlling single and multiple lane load distribution factors, respectively. The 102 bridges consisted of bridges with longer span lengths of 100 feet, overhang dimensions of zero to three feet, and various timber moduli of elasticity. The majority of the bridges analyzed were based on the Standard Plans for Timber Highway Structures [10] and consisted of geometries in the following range:

- Clear width varied from 12'-0" to 36'-0"
- Span length varied from 20'-0" to 80'-0"
- Girder spacing varied from 3'-4" to 6'-0"
- Overhang dimensions, from the face-of-curb to the center of the exterior girder, varied from 12 inches to 30 inches.

The analytical results from the bridges above were compared to the current 2005 AASHTO LRFD live load distribution factors. The AASHTO LRFD live load distribution equations consist of the "S/D" equation and the lever rule. From these results, one can observe the need for equations with greater accuracy. The objective was to develop equations with greater accuracy, while maintaining a level of simplicity. Based on performance, the parametric equations and the lever rule were recommended. The parametric equations contain constants known during the preliminary design phase. The parametric equations were developed using the regression analysis solver provided in Microsoft Excel.

To adjust for any inherent variability, the developed parametric equations were adjusted using the affine transformation process and the distribution simplification factor, similar to

NCHRP 12-62 [11]. These statistical adjustments shift the mean of the proposed equation results to produce conservative values when compared to the finite element results.

Limitations of the proposed equations

The proposed equations do have limitations. These limitations are based on the assumptions and parameters used to create the proposed equations. The proposed equations meet the conditions already established by the AASHTO LRFD [2] specification and they are as follows:

- Width of the deck is constant.
- Unless otherwise specified, the number of beams is not less than four.
- Beams are parallel and have approximately the same stiffness.
- Unless otherwise specified, the roadway part of the overhang, d_e, does not exceed 3.0 ft.
- Curvature in plan is less than the limit specified in article 4.6.1.2.
- Cross-section is consistent with that of a glued-laminated timber girder bridge with glued-laminated timber deck panels provided by AASHTO.

For simplification, the proposed equations do not consider bridges on a skew, with a sidewalk, and the influence of diaphragms. The equations are limited to bridges with one to two traffic lanes. The proposed live load distribution equations will produce accurate results when within the geometries listed previously.

Recommendations

Based on the analytical modeling and the comparison of the results above, the following can be recommended:

1. The proposed distribution equations were created for glued-laminated timber girder bridges with glued-laminated timber deck panels only. Similar live load distribution factors should be considered for additional timber bridge types.
2. The proposed equations decrease slightly in accuracy for bridges pushing the limits of the parametric bridges. Wittson Bridge is an example of a bridge pushing the limits of the span length boundaries used to develop the live load distribution equations in this report. For bridges pushing the limits of the equations, the multiple presence factors should remain unaltered. This will aid in producing conservative results.
3. The shear live load distribution equations developed in this report account for the controlling shear design values. The need for Eq. 1 above should be reviewed. This equation is used to investigate shear parallel to the grain of the glulam girders and increases the distributed shear load determined with the existing AASHTO LRFD live load distribution factors.
4. Further comparisons of the developed live load distribution equations to additional field test data is recommended for further validation of the equations.

CHAPTER 3. LIVE LOAD DISTRIBUTION ON LONGITUDINAL GLUED LAMINATED TIMBER DECK BRIDGES

Abstract

Over the past few years the United States Department of Agriculture (USDA) - Forest Products Laboratory (FPL) and the Federal Highway Administration (FHWA) have supported several research programs. This report is a result of a study sponsored by the FPL, with the objective of determining how truckloads are distributed to the deck panels of a longitudinal glued-laminated timber deck bridge. Currently, the American Association of State Highway and Transportation Officials (AASHTO) LRFD Bridge Design Specification provides live load distribution provisions for longitudinal glued-laminated timber deck panel bridges.

The AASHTO LRFD live load distribution provisions for longitudinal glued-laminated timber deck bridges were based on the assumption that the bridge deck behaves as one slab, i.e. ignoring the discontinuity of the bridge deck panels. This report investigates this assumption by utilizing analytical models that were validated using field test data from several in-service bridges and data from a full-scale laboratory test bridge. The analytical models accounted for the effects of the interface between the deck panels as well as the effects of the transverse stiffener beams on the distribution of the live load. The analytical live load distribution results above were compared to both the AASHTO LRFD and AASHTO Standard Specifications.

Objective and Scope

The overall objective of the study presented herein was to evaluate how an applied truck load is distributed among the deck panels of the longitudinal glued-laminated timber deck bridge system. This evaluation was attained by utilizing test data from several in-service bridges,

laboratory test bridges, and analytical results. These results were compared to the 2005 AASHTO LRFD and 1996 AASHTO Standard Specification live load distribution provisions for longitudinal glued-laminated timber deck bridges.

The objectives listed above were accomplished by completing the following five tasks:

1. Review the American Association of State Highway and Transportation Officials (AASHTO) Bridge Design Specifications and the associated load distribution criteria for longitudinal glued-laminated timber deck bridges. This review included both the AASHTO LRFD and AASHTO Standard Specifications.
2. Develop detailed analytical finite element models to evaluate the structural performance of the longitudinal glued-laminated timber deck bridges. These analytical models account for the orthotropic behavior of timber material, the interface between the deck panels, and the deck panel stiffener beam interaction.
3. The finite element results were validated by comparing the analytical results of the deck panel deflections and live load distribution values to the data attained from the field tests of the in-service bridges that were conducted by researchers at ISU.
4. Study the influence of other parameters such as the interface between the deck panels, stiffener beam spacing, and the stiffener beam size on the distribution of live load.
5. If required, develop live load distribution formulas. These formulas should be based on simplified methods or parametric equations using variables that are known during preliminary design.

Background

Simple live load distribution equations have appeared in the AASHTO Standard Bridge

Design Specifications for many years. However, the AASHTO LFRD Bridge Design Specification introduced major revisions to the live load distribution provisions for slab type bridges. Longitudinal glued-laminated timber deck panel bridges with spreader beams were included in these revisions.

The 1996 AASHTO Standard Specification [1] live load distribution factors for longitudinal glued-laminated timber deck bridges were presented based on wheel loads, or half of the total axle load, carried by a single panel. The equations used for flexure design are listed in Table 23 for a panel under single or multiple truck loads. The AASHTO Standard Specification requires one stiffener beam to be placed at mid-span with all other stiffener beams placed at intervals of 10 feet or less. These stiffener beams are attached near the edges of the deck panels, typically with a bolted connection, and should have a stiffness of 80,000 kip-in^2 or greater [1].

Table 23. 1996 AASHTO Standard Specification, Wheel Load Distribution Factors [1]

Design Loading	Equation for Flexure
One Traffic Lane	$\frac{W_p}{4.25+\frac{L}{28}}$ or $\frac{W_p}{5.50}$ whichever is greater
Two Traffic Lanes	$\frac{W_p}{3.75+\frac{L}{28}}$ or $\frac{W_p}{5.00}$ whichever is greater

(From AASHTO 3.25.3)

Where,

W_p = Width of panel (feet) ($3.5 \leq W_p \leq 4.5$)

L = Length of bridge, center of bearing to center of bearing (feet)

The 2005 AASHTO LRFD Bridge Design Specification [2] provides equivalent strip width equations for longitudinal glued-laminated timber deck bridges. The equivalent strip width equations are based on lane loads, or full axle loads as shown in Table 24 below. These

equations are also used to design reinforced concrete slab bridges and post tensioned timber deck bridges. The AASHTO LRFD Specification requires one stiffener beam to be placed at intervals of 8 feet or less. The stiffener beam is connected with a through bolt connection to the deck near the panel edges and should have a stiffness of 80,000 kip-in^2 or greater [2].

Table 24. 2005 AASHTO LRFD Design Specification, Equivalent Width Equations [2]

Design Loading	Moment Equation
One Traffic Lane	$E=10.0+5.0\sqrt{L_1 W_1}$
Two or more Traffic Lanes	$E=84.0+1.44\sqrt{L_1 W_1} \leq \frac{12.0W}{N_L}$

(From AASHTO 4.6.2.3)

Where,

E = Equivalent width (inches)

L_1 = Modified span length taken to the lesser of the actual span or 60 (feet)

W_1 = Modified width of the bridge taken to be equal to the lesser of the actual width or 60.0 for multilane loading, or 30.0 for single-lane loading (feet)

W = Physical edge-to-edge width of bridge (feet)

N_L = Number of design lanes

Multiple presence factors are included in the AASHTO Standard and LRFD Specification equations that are listed in Table 23 and Table 24 respectively. These factors account for the uncertainties associated with the number of loaded lanes and are shown in Table 25. For example, for bridges with multiple design lanes it is unlikely three adjacent lanes will be loaded at the same time. Therefore, the design load is decreased. For the single design lane condition, the AASHTO LRFD multiple presence factor is greater than one to account for an overload condition [2].

Table 25. AASHTO Multiple Presence "m" Factors

Number of Loaded Lanes	AASHTO Standard Specification [1]	2005 AASHTO LRFD [2]
1	1.0	1.2
2	1.0	1.0
3	0.9	0.85
> 3	0.75	0.65

Literature Review

The 1996 AASHTO Standard Specification live load distribution provisions for longitudinal glued-laminated timber deck bridges, Table 23, were based on research performed by Sanders et. al. [20]. Sanders et. al. performed analytical studies to determine the load distribution characteristics of longitudinal glued-laminated timber deck bridges. The analytical models were created using SAP IV finite element software. In their work, Sanders et. al. [20] used plate elements to model the deck panels and beam elements to model the stiffener beam. These elements were connected using rigid links. With the finite element model, parametric studies were preformed on bridges with span lengths from 9 to 33 feet, roadway widths from 16 to 40 feet, deck thickness from 6.75 to 12.25 inches, and various stiffener beam arrangements. Additionally, the width of the deck panels were varied from 42 to 54 inches [20].

Research of the longitudinal glued-laminated timber deck bridges was also conducted by Funke et. al. [19]. This research consisted of laboratory testing and analytical finite element modeling using SAP IV finite element software. The laboratory experiments were performed on full-scale bridges with a span length of 26 feet. Various stiffener beam, deck panel, and load positioning arrangements were utilized in the laboratory testing. The laboratory results from this study verified the applicability of the live load distribution equations created by Sanders et. al. [20]. Favorable live load distribution behavior occurred when using at least three stiffener beams.

In the 1980's the National Cooperative Highway Research Program (NCHRP) Project 12-26, Zokaie T. et.al. [18] developed live load distribution equations for slab bridges. The live load distribution equations documented in the NCHRP 12-26 report were the basis of the load distribution provisions presented in the 2005 AASHTO LRFD Design Specifications. To develop equations with a wide range of applicability, a large database of bridges with various parameters were selected. The database consisted 130 reinforced concrete slab bridges. Longitudinal glued laminated timber deck bridges were not considered in NCHRP Project 12-26 [18].

Zokaie T. et.al. [18], utilized grillage models to evaluate the 130 reinforced concrete slab bridges. From these results, the authors of NCHRP 12-26 developed relationships to calculate the equivalent strip width equations provided in Table 24 using grillage models. The grillage mesh consists of longitudinal and transverse beam elements. Load distribution factors were determined for each of the longitudinal beam elements, similar to the method used for girder-slab bridges. Dividing the load distribution factor by the width of the deck represented by the longitudinal beam element in the grillage model produces a moment distribution factor per unit width. The load distribution design width, or equivalent strip width, is determined by taking the inverse of this factor. Simply, the equivalent strip width values can be determined using Eq. 1 below. This equation allows one to relate live load distribution factors to equivalent strip widths. Edge stiffening effects from guardrails, or barriers, were not included in the analysis [18].

$$E_i = \frac{W_E}{DF_i} \tag{1}$$

Where,

DF_i = Lane load distribution factor of the *i*th longitudinal beam.

E_i = Equivalent strip width of the *i*th longitudinal beam, inches.

W_E = Tributary width of longitudinal beam element.

Several analytical studies were performed on longitudinal glued-laminated timber deck bridges at Iowa State University in recent years. Kurian [9] conducted finite element analyses to investigate the effects of several design parameters on the overall structural behavior of many in-service bridges. The parametric analyses performed by Kurian [9] examined the effects of edge stiffening, boundary conditions, and the change in the timber modulus of elasticity. Kurian [9] concluded that the modulus of elasticity had a significant influence on bridge response when comparing the deflections attained from the analytical models to the field test results. Kurian [9] also noted the influence of edge stiffening becomes insignificant to the panel deflections and stresses moving from the exterior panels to the interior panels. This study focused only on deflection results and did not address load distribution.

Analysis of longitudinal glued-laminated timber deck bridges

The results reported herein were attained from detailed finite element analyses. These analyses were carried out using ANSYS [3], ANSYS is a general-purpose finite element program and was used to calculate deflections, stresses, and strains that are induced in several in-service longitudinal glued-laminated timber deck panel bridges under various truck loadings. To facilitate the construction of multiple finite element models, of various timber bridges, it was necessary to develop a preprocessor that simplifies the generation of such models. For this purpose, the ANSYS parametric design language (APDL) was utilized to write the needed preprocessor. The preprocessor was developed to allow users with limited finite element analysis knowledge to model longitudinal glued-laminated timber deck bridges. The preprocessor program utilizes the information entered by the user to generate the finite element model, as shown in Figure 42.

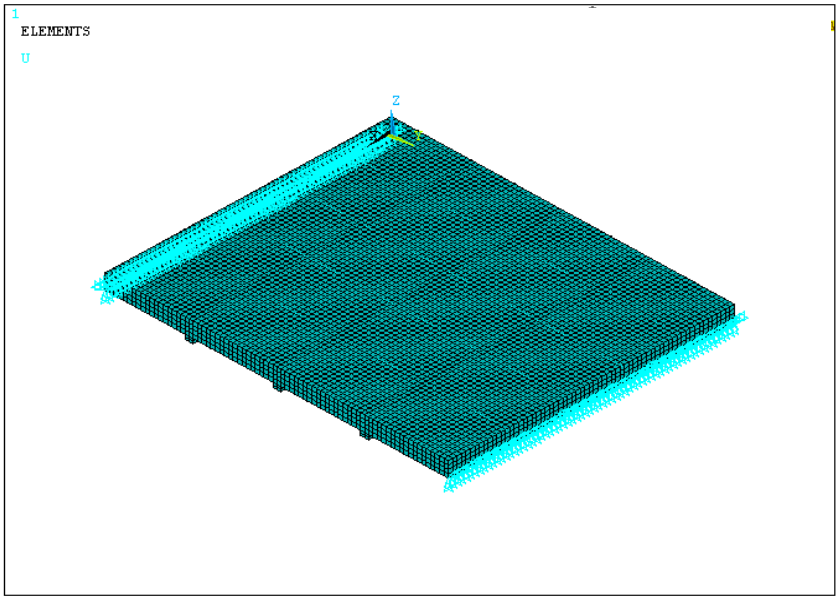

Figure 42. Three Dimensional Rendering of the Finite Element Model

To execute the preprocessor the user needs to provide input parameters such as the span length, deck panel width, deck panel thickness, material properties, truckloads, and the boundary conditions. In addition, the finite element model constructed with the preprocessor allowed the user to model the longitudinal glued-laminated timber deck bridges as either one single deck panel or with individual deck panels. The deck panels may act as one single panel due to swelling of the deck panels. When modeling the individual deck panels, the program allowed the user to adjust the stiffness of the interface elements between the deck panels. This was accomplished by connecting the interface between the deck panels with nonlinear spring elements. The nonlinear spring elements allow the user to adjust the interaction of the deck panels by defining different coefficient of friction values to model the normal and sliding forces acting between the panels.

The finite element model utilized solid "brick" elements to model the timber deck panels as well as the stiffener beam. This element allows one to incorporate the orthotropic timber

material properties in the longitudinal (L), radial (R), and tangential (T) directions. The longitudinal modulus of elasticity is typically known. The orthotropic timber properties, related to the longitudinal modulus of elasticity, used for this report were provided in the FPL 1999 Wood Handbook [7]. The FPL 1999 Wood Handbook [7] provides the twelve constants required to represent the orthotropic properties of timber. The selected timber species was Douglas-Fir, which is a typical softwood species used for glued-laminated timber beams.

The stiffener beam interaction with the deck panels varies over the width of the bridge. For this purpose, compression only spring elements were used to idealize the interface between the panels and the stiffener beam. The stiffness of the spring element becomes zero when a gap exists between the deck panel and the stiffener beam. Additionally, tension-compression spring elements were utilized to model the through bolt, or aluminum bracket, connections that are required to connect the stiffener beam to the deck panels. The load displacement relationships of these connections, in tension, were determined from experimental test data provided by the Weyerhaeuser Company, Tacoma (unpublished data) [25]. The stiffness of the through bolt and aluminum bracket connections, when in compression, were assumed to be large i.e. to act as a rigid connection. The tension-compression relationships of the aluminum bracket and through bolt connections are shown in Figure 43.

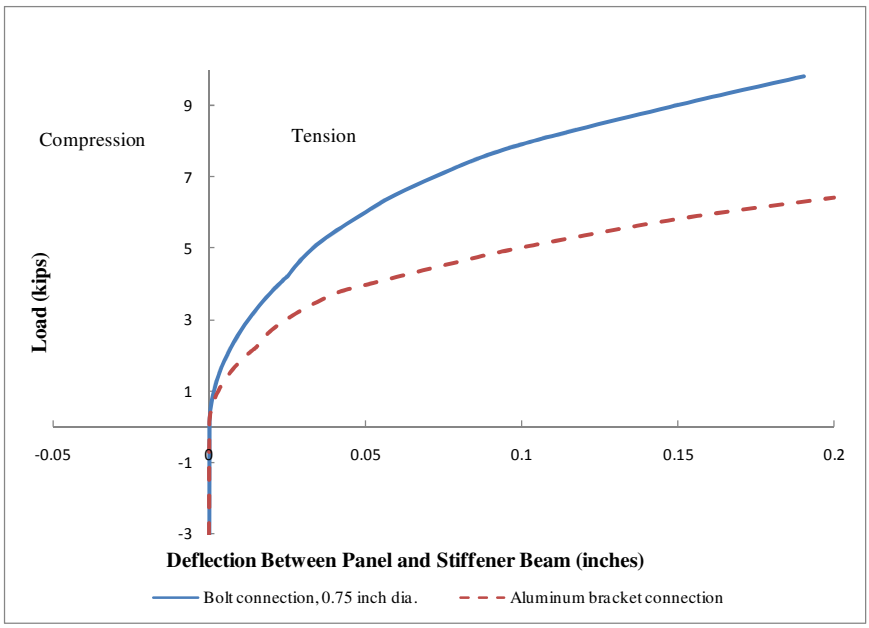

Figure 43. Load Deflection Data Used in the Finite Element Analysis, from [18]

Analysis of in-service bridges

General

As previously mentioned, several in-service and laboratory longitudinal glued-laminated timber deck bridges were tested by ISU researchers. The collected data from these tests consisted of deflections that were recorded at the edge of each deck panel. Longitudinally, these deflections were measured at, or near, the mid-span of each deck panel edge. The live load distribution factors of the in-service bridges, for each panel, were determined using Eq. 2 below [8]. In the work presented herein, these in-service live load distribution results were compared to the AASHTO Standard and LRFD live load distribution provisions. Additionally, the in-service deflection and live load distribution results were compared to the values attained using the finite element preprocessor described above.

$$DF_i = \frac{\Delta_i}{\sum_{i=1}^{n} \Delta_i} \tag{2}$$

Where,

Δ_i = Average deck panel deflection

DF_i = Lane load distribution fraction of the *i*th panel

$\sum\Delta_i$ = Sum of average panel displacement

n = Number of panels

Angelica Bridge

Angelica Bridge located in the Town of Angelica, New York State was tested by ISU researchers in 1996 and 2003 [21]. The field test results presented herein were based on the 2003 results. This bridge has a span length of 21'-4", a clear width of 28'-3", and consists of seven glued-laminated deck panels. The deck panels have a width of 4'-2" and a depth of 8.25 inches. This bridge has two stiffener beams that are spaced at 7'-6". The two stiffener beams are 6.875 inches wide and have a depth of 8.25 inches. The stiffener beams were connected to the deck panels using through bolts. The asphalt wearing surface on the deck panels was 2.5 inches thick.

The worst-case deflections and live load distribution factors from the field test results were created when the test vehicle is located near the guard rail. As the truck moved transversely towards the center of the bridge, the deflection and live load distribution values would decrease. The controlling deflection results were created from the load case shown in Figures 44a and 44b. The test vehicle configuration is shown in Figure 45.

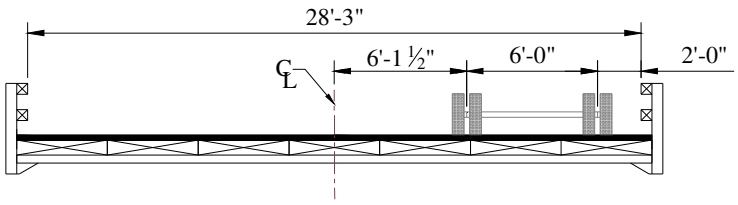

Figure 44a. Controlling Transverse Load Position for Angelica Bridge

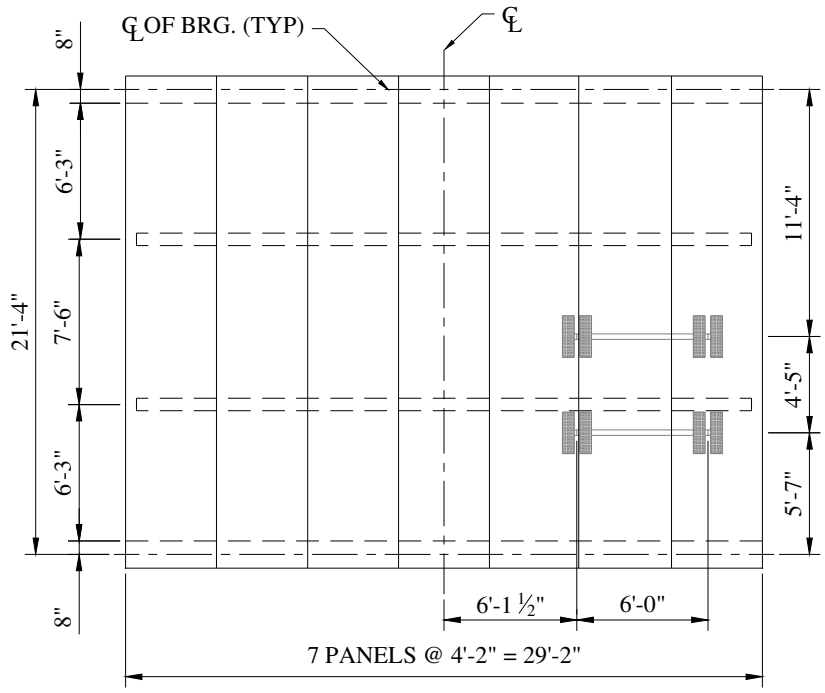

Figure 44b. Controlling Load Position for Angelica Bridge, Plan Veiw

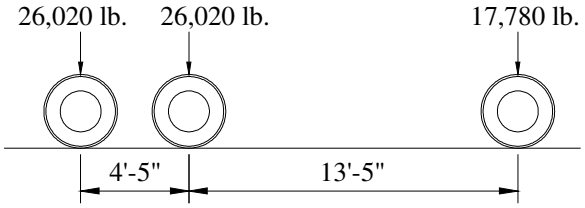

Figure 45. Angelica Bridge, Test Vehicle Axle Configuration

The field test deflection results, from the load position above, were compared to the results attained using the finite element program described previously. Initially the bridge was modeled with individual deck panels. However, this idealization resulted in larger overall deflections than those obtained from the field test. Notice from Figure 46, the field test results show minimal differential displacements between two adjacent deck panels. The maximum differential displacement between the panels is 0.037 inches. Due to the small differential panel

displacements, the bridge was then modeled as a single deck panel. A combination of the swelling of the deck panels, close spacing of the stiffener beams, and the presence of the asphalt wearing surface could be the reason the bridge behaves as a single panel.

The finite element results obtained from modeling the deck as a single panel are shown in Figure 46. The effect of the asphalt wearing surface was included in the analysis by assuming the timber deck panel and the asphalt act compositely. Using strain compatibility, the modular ratio of the asphalt and the timber deck panels, the thickness of the deck panels was increased by 0.75 inches. The guard railing consisted of timber posts and timber rails, but they were not explicitly included in the finite element model. From the deflection results, one can observe that the guard rail system had minimal influence on the exterior panel deflection values. Therefore, no adjustment was made to account for the influence of the guard rail system. The finite element deflection results compared well to the field test results when modeling the as-built deck thickness, or when accounting for the asphalt wearing surface.

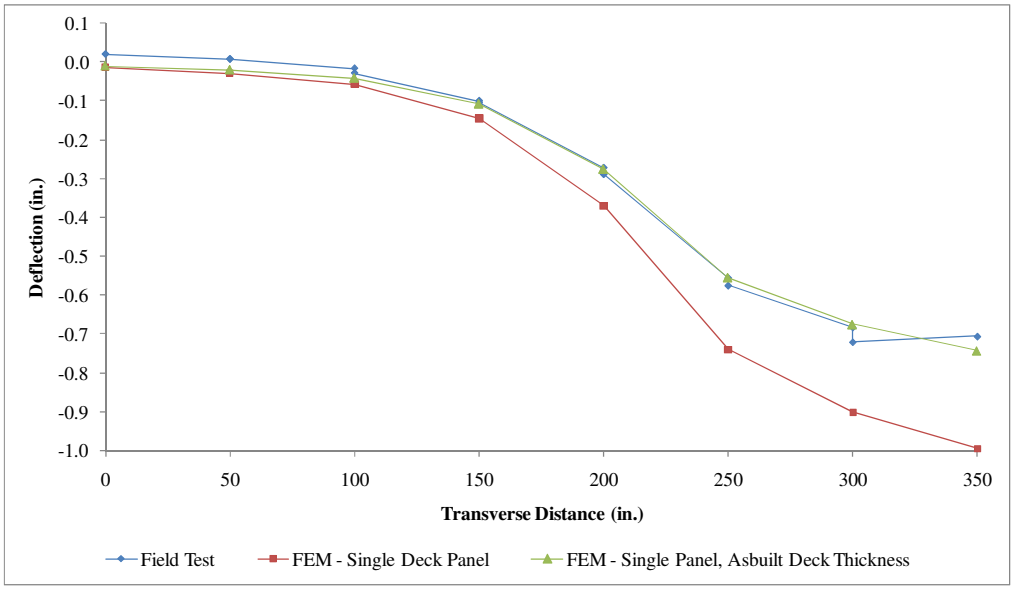

Figure 46. Angelica Bridge Deflection Results

The live load distribution factor results for Angelica Bridge are shown in Figure 47 below. For comparison to the field test and finite element results, the 2005 AASHTO LRFD equivalent strip values would need to be converted to live load distribution factors per panel. From Table 24, the equivalent strip width equation for a longitudinal glued laminated timber deck bridge under a single truck load is:

$$E = 10.0+5.0\sqrt{(L_1)(W_1)} \quad (3)$$

Substituting the bridge length and width for Angelica Bridge into Eq. 3, one will get the following equivalent strip width value:

$$E = 10.0+5.0\sqrt{(21.33)(28.25)} = 132.74 \text{ in.} \quad (4)$$

This equation includes the 1.2 multiple presence factor per the AASHTO LRFD Specification [2]. To remove the multiple presence factor, one must multiply the equivalent strip width value from above by 1.2:

$$E_{adj} = 132.74\ (1.2) = \ 159.28 \text{ in.} \quad (5)$$

Rearranging the equivalent strip width and distribution factor relationship provided in Eq. 1, provides Eq. 6 below:

$$DF = \frac{W_E}{E_{adj}} \quad (6)$$

Where,

DF = Lane load distribution factor converted from AASHTO LRFD equivalent strip width.

E_{adj} = Equivalent strip width the multiple presence factor removed.

W_E = Tributary width longitudinal beam element, or width of the panel

Using Eq. 6, one can determine the AASHTO LRFD lane load distribution factor for the width of the panel to be:

$$\text{DF} = \frac{50 \text{ in}}{159.28 \text{ in}} = 0.313 \quad \text{(without 1.2 multiple presence factor)}$$

Figure 47 summarizes the Angelica Bridge live load distribution results for the load case shown in Figure 44. The finite element single panel live load distribution factor results compare well to the field test results. Accounting for effects of the wearing surface had minimal influence on the finite element live load distribution results. Both the finite element and the field test results exceed the limits set by the AASHTO LRFD Specification when the multiple presence factor is removed. However, with the inclusion of the single lane multiple presence factor, the AASTHO LRFD Specification does provide conservative results. The exterior panel live load distribution results are provided in Table 26.

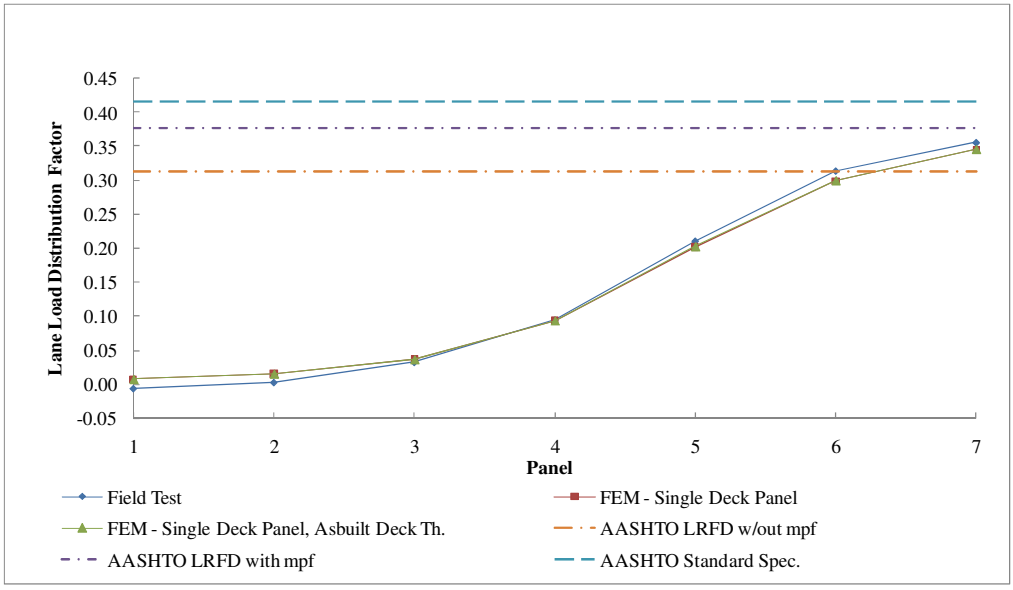

Figure 47. Angelica Bridge Lane Load Distribution Factor Results

Table 26. Angelica Bridge, Live Load Distribution Factors

Exterior panel live load distribution results	
Field test =	0.356
FEM - Single deck panel =	0.345
AASHTO Standard Spec =	0.416
AASHTO LRFD with mpf =	0.376
AASHTO LRFD without mpf =	0.313

East Main Street Bridge

East Main Street Bridge located in the Town of Angelica, New York State was tested by ISU researchers in 1996 and 2003 [22]. The field test results presented herein were based on the 2003 results. The bridge has a span length of 30'-6", a clear width of 34'-0", and consists of eight glued-laminated deck panels. The deck panels have a width of 4'-5" and a depth of 14.25 inches. This bridge has four stiffener beams, which are spaced at 6'-0". The stiffener beams are 6.875 inches wide and have a depth of 4.5 inches. The stiffener beams were connected to the deck panels with through bolts. The asphalt wearing surface is 3.0 inches thick. The worst-case deflections and live load distribution factors from the field tests were created from the load case shown in Figures 48a and 48b. The test vehicle configuration is the same as shown in Figure 45.

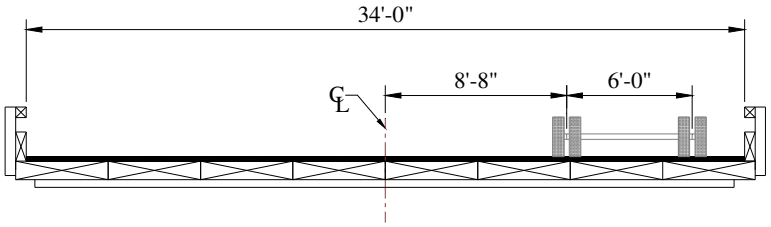

Figure 48a. Controlling Transverse Load Position for East Main Street Bridge

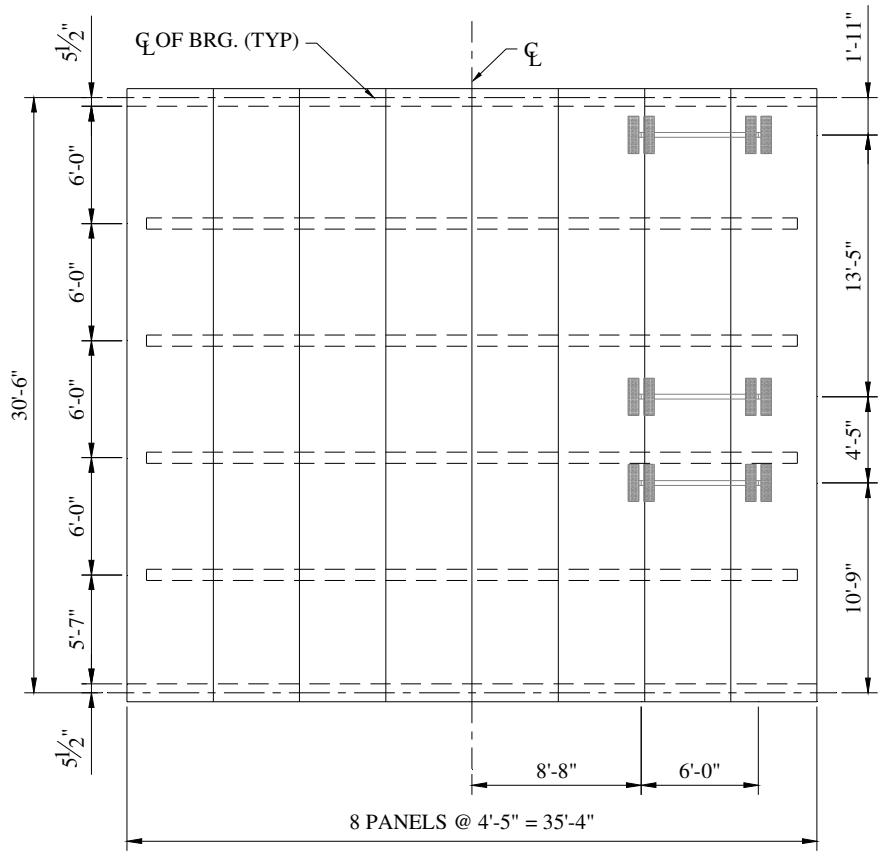

Figure 48b. Controlling Load Position for East Main Street Bridge, Plan View

The deflection and live load distribution factors for East Main Street Bridge are shown in Figures 49 and 50, respectively. These results are based on the load condition shown in Figures 48a and 48b. Unlike the previous bridge, edge stiffening effects were observed in the exterior panels. Further adjustments were made to the finite element as-built deck thickness results, incorporating edge stiffening effects. This was accomplished using the results published by Kurian [9]. The adjustment was made by reducing the deflections using the difference between the results obtained with and without the railing system as documented by Kurian [9]. Similar to the previous bridge, the AASHTO LRFD equivalent strip width values, with and without the multiple presence factor, were converted to a distribution factor. The controlling exterior panel

live load distribution results are provided in Table 27. In addition, the AASHTO Standard Specification live load distribution factors, from Table 23, were included in the results below for East Main Street Bridge.

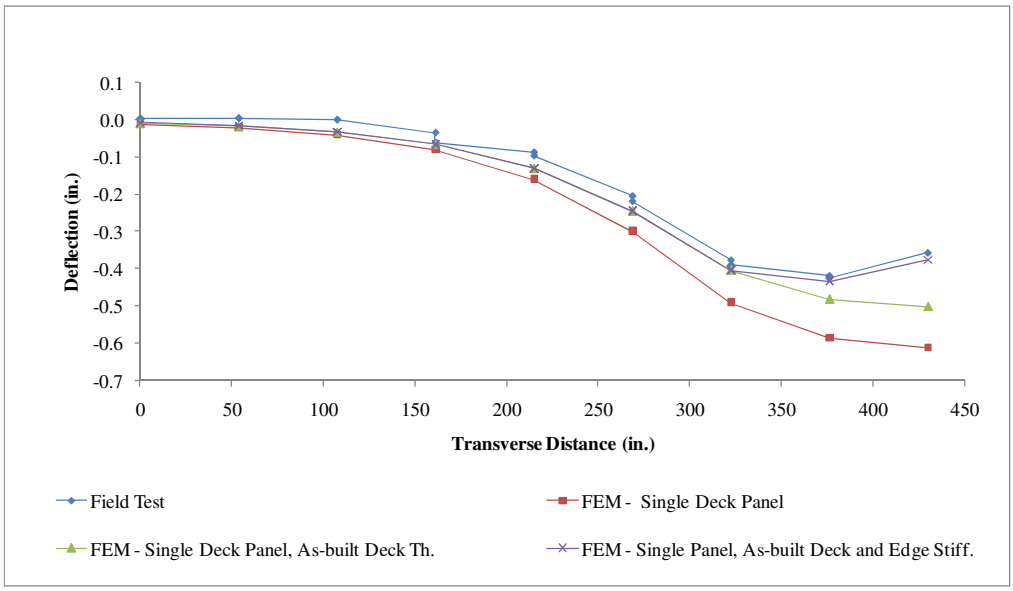

Figure 49. East Main Street Bridge Deflection Results

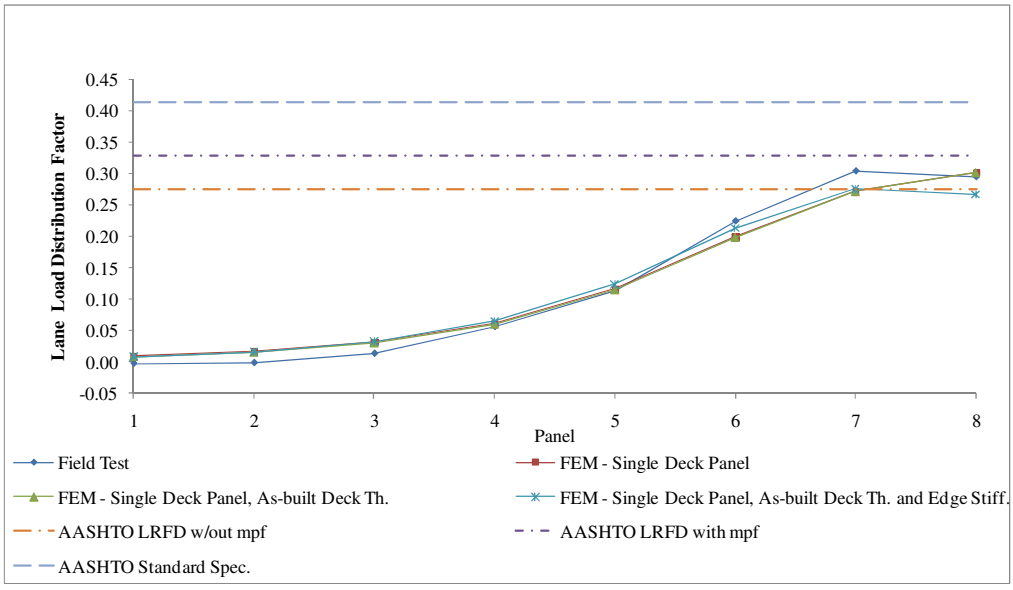

Figure 50. East Main Street Bridge Lane Load Distribution Results

Table 27. East Main Street Bridge, Live Load Distribution Factors

Exterior panel live load distribution results	
Field test =	0.304
FEM - Single deck panel =	0.301
AASHTO Standard Spec =	0.414
AASHTO LRFD with mpf =	0.329
AASHTO LRFD without mpf =	0.274

Bolivar Bridge

Bolivar Bridge located in the Town of Angelica, New York State was tested by ISU researchers in 1996 and 2003 [23]. The field test results presented herein were based on the 2003 results. The bridge has a span length of 28'-8", a clear width of 24'-8", and consists of six glued-laminated deck panels. The deck panels have a width of 4'-5" and a depth of 15.0 inches. This bridge has three stiffener beams that are spaced at 7'-6". The two stiffener beams are 6.875 inches wide and have a depth of 4.5 inches. The stiffener beams were connected to the deck panels with through bolts. The asphalt wearing surface is 2.5 inches thick. The effect of the wearing surface was included in the analysis, as explained above. The guard railing system consisted of timber posts and a glued-laminated timber panel barrier, they were not explicitly included in the finite element model. The worst-case deflections and live load distribution factors from the field test results were created from the load case shown in Figures 51a and 51b. The test vehicle configuration is the same as shown in Figure 45.

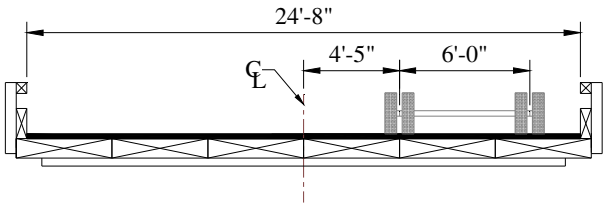

Figure 51a. Controlling Transverse Load Position for Bolivar Bridge

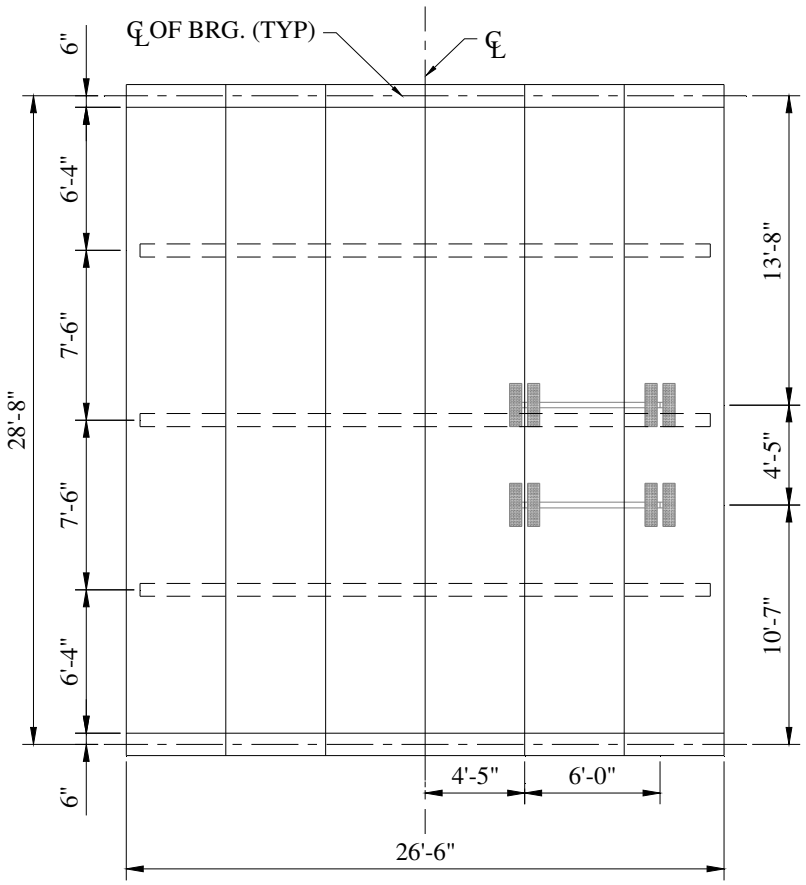

Figure 51b. Controlling Load Position for Bolivar Bridge, Plan View

The deflection and live load distribution factors for Bolivar Bridge are shown in Figures 52 and 53, respectively. These results are based on the load condition shown in Figures 51a and 51b. Edge stiffening effects were observed in the exterior panels and the deflections were adjusted as described previously. As before, the AASHTO LRFD equivalent strip width values, with and without the multiple presence factor, were converted to distribution factors. The controlling exterior panel live load distribution results are provided in Table 28.

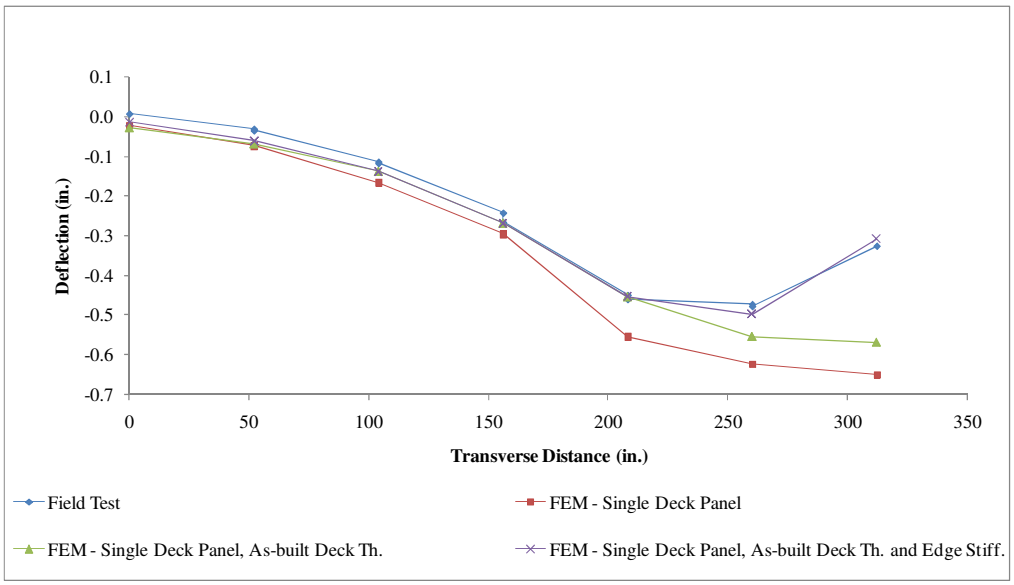

Figure 52. Bolivar Bridge Deflection Results

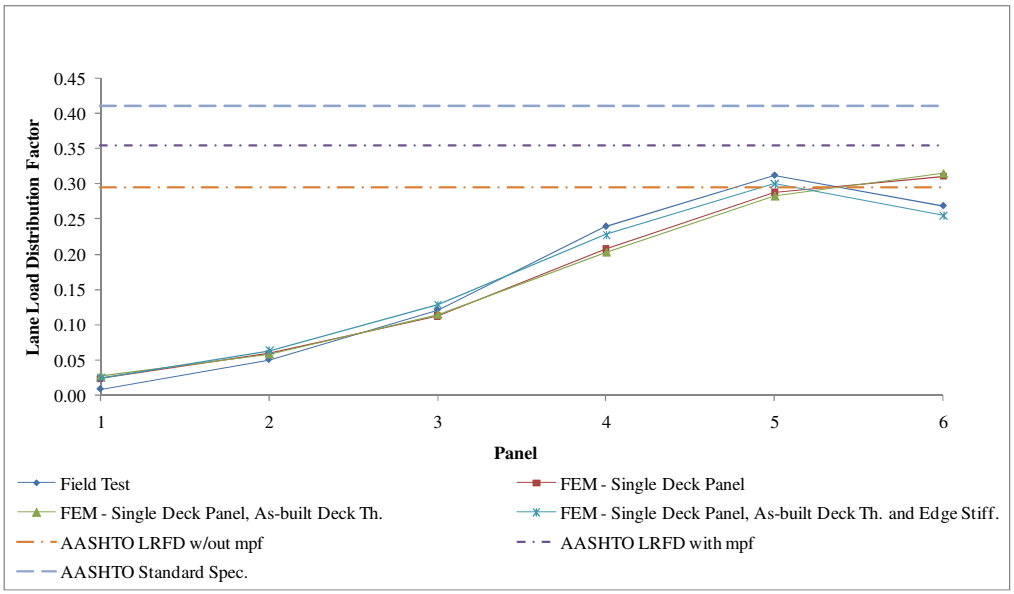

Figure 53. Bolivar Bridge Lane Load Distribution Factor Results

Table 28. Bolivar Bridge, Live Load Distribution Factors

Exterior panel live load distribution results	
Field test =	0.312
FEM - Single deck panel =	0.310
AASHTO Standard Spec =	0.411
AASHTO LRFD with mpf =	0.355
AASHTO LRFD without mpf =	0.296

Scio Bridge

Scio Bridge located in the Town of Angelica, New York State was tested by ISU researchers in 1996 and 2003 [24]. The field test results presented herein were based on the 2003 results. The bridge has span length of 20'-8", a clear width of 30'-0", and consists of six glued-laminated deck panels. The deck panels have a width of 4'-4" and a depth of 9.0 inches. This bridge has three stiffener beams that are spaced at 7'-6". The two stiffener beams are 6.875 inches wide and have a depth of 4.5 inches. The stiffener beams were connected to the deck panels with the through bolt connection. The asphalt wearing surface is 6.0 inches thick. The effect of the wearing surface was included in the analysis, as explained above. The guard railing system consisted of timber posts and a glued-laminated timber panel barrier. The worst-case deflections and live load distribution factors from the field test results were created from load case shown in Figure 54. The test vehicle configuration is the same as shown in Figure 45.

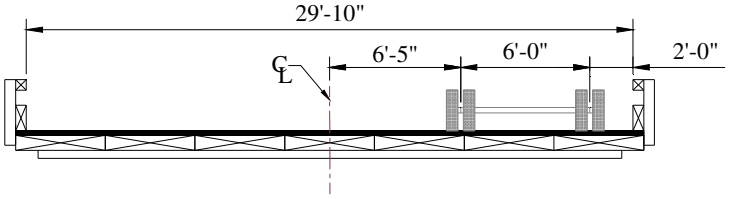

Figure 54a. Controlling Transverse Load Position for Scio Bridge

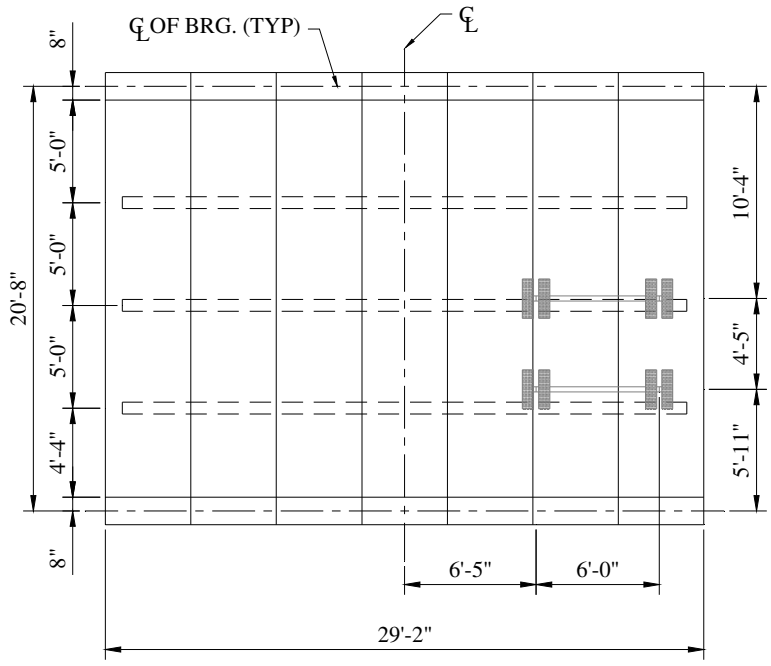

Figure 54a. Controlling Load Position for Scio Bridge, Plan View

The deflection and live load distribution factors for Scio Bridge are shown in Figures 55 and 56, respectively. These results are based on the load condition shown in Figures 54a and 54b. Edge stiffening effects were observed in the exterior panels and the deflections were adjusted as described previously. As before, the AASHTO LRFD equivalent strip width values, with and without the multiple presence factor, were converted to distribution factors. The controlling exterior panel live load distribution results are provided in Table 29.

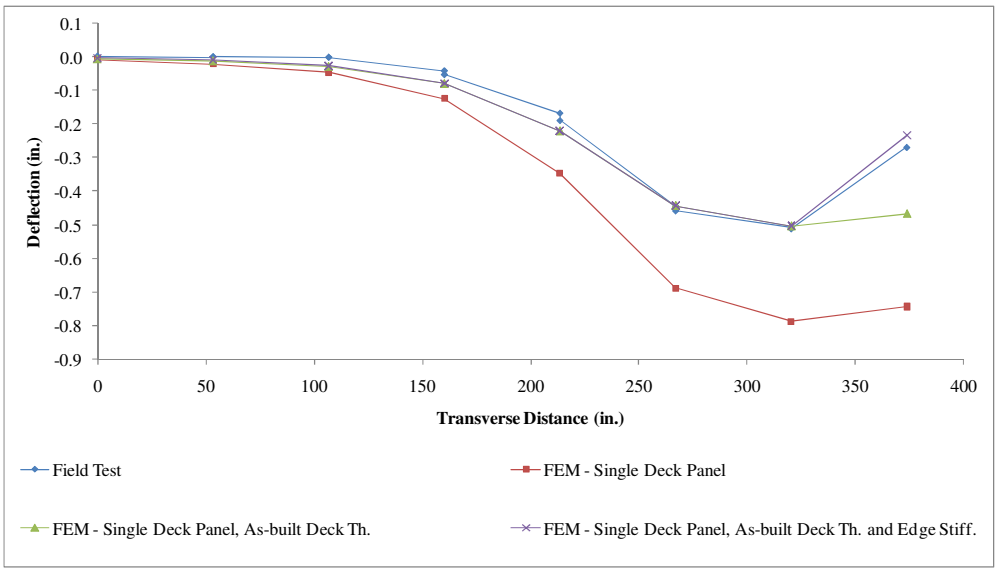

Figure 55. Scio Bridge Deflection Results

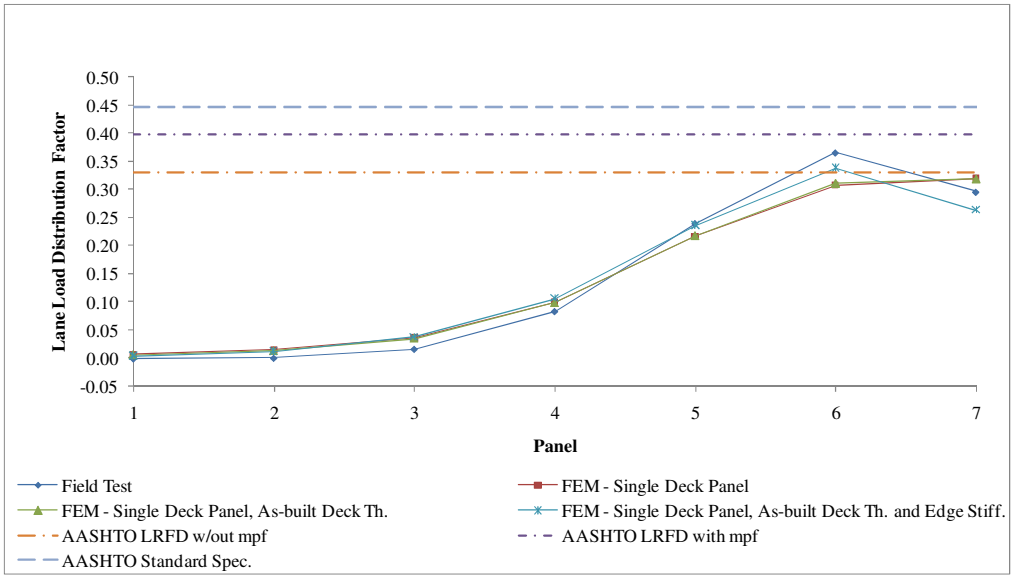

Figure 56. Scio Bridge Lane Load Distribution Results

Table 29. Scio Bridge, Live Load Distribution Factors

Exterior panel live load distribution results	
Field test =	0.366
FEM - Single deck panel =	0.338
AASHTO Standard Spec =	0.447
AASHTO LRFD with mpf =	0.398
AASHTO LRFD without mpf =	0.331

Analysis of the Laboratory test bridge

General

The full-scale laboratory test bridge allows one to study the behavior of the longitudinal glued-laminated timber deck panel bridge without the influence of swelling, the asphalt wearing surface, and edge stiffening effects from guardrails or barriers. The laboratory test bridge had a span length of 26'-0". This bridge set-up consisted of six deck panels with one stiffener beam located at the mid-span of the bridge. The deck panels were 4'-0" wide and had an average depth of 10.72 inches. The stiffener beam had a depth of 4.5 inches and a width of 6.75 inches. The stiffener beam was connected to the deck panels with the through bolt connection described earlier. The load consists of a single HS20-44 design truck placed 30 inches from the edge of the deck as shown in Figure 57. Longitudinally, two axles were placed on the bridge. One axle was placed 2'-6" from the center line of the abutment and the other axle was placed 14'-0" from the first.

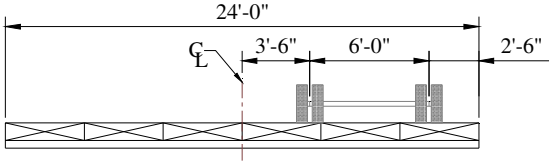

Figure 57. Laboratory Test Bridge ITE6-A

The laboratory bridge [19] was analyzed as having individual deck panels and as one single deck panel. When modeling the bridge with the individual deck panels, the nonlinear spring elements connecting the deck panels were assigned negligible coefficient of friction and stiffness values, allowing the deck panels to slide freely. Therefore, the stiffener beam was the only component transferring load from panel to panel. As mentioned above, the stiffener beam was connected to the deck panels with through bolts. Therefore, the compression-tension force

verses displacement values for the through bolt connection, shown in Figure 43, were utilized by the preprocessor described above.

The finite element displacement results compared well to the laboratory test displacement results and are provided in Figure 58. The individual deck panel finite element results are within a two percent difference of the laboratory displacement results. The live load distribution factor results of the laboratory test bridge, finite element analyses, and AASHTO LRFD and Standard Specifications are shown in Figure 59. One can observe the controlling live load distribution factor is located at the exterior panel. The individual deck panel finite element results are within a two percent difference of the laboratory live load distribution results. The controlling live load distribution factor from the single panel model compared well to the AASHTO LRFD live load distribution value with the multiple presence factor removed. The individual deck panel finite element and field test results compared well to the AASHTO Standard specification limit shown in Figure 59.

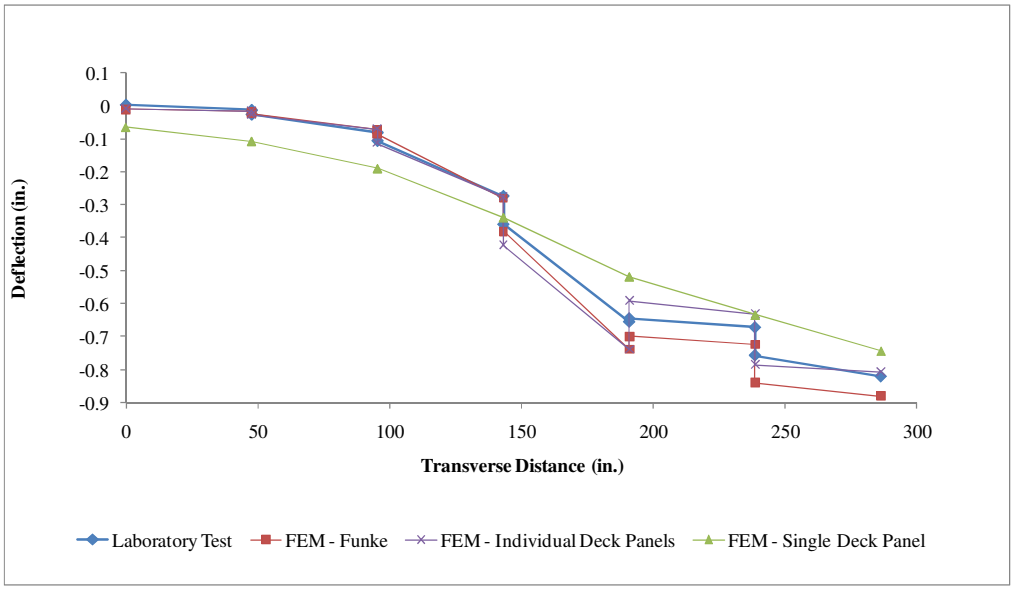

Figure 58. Laboratory Test Bridge ITE6-A, Deflection Results

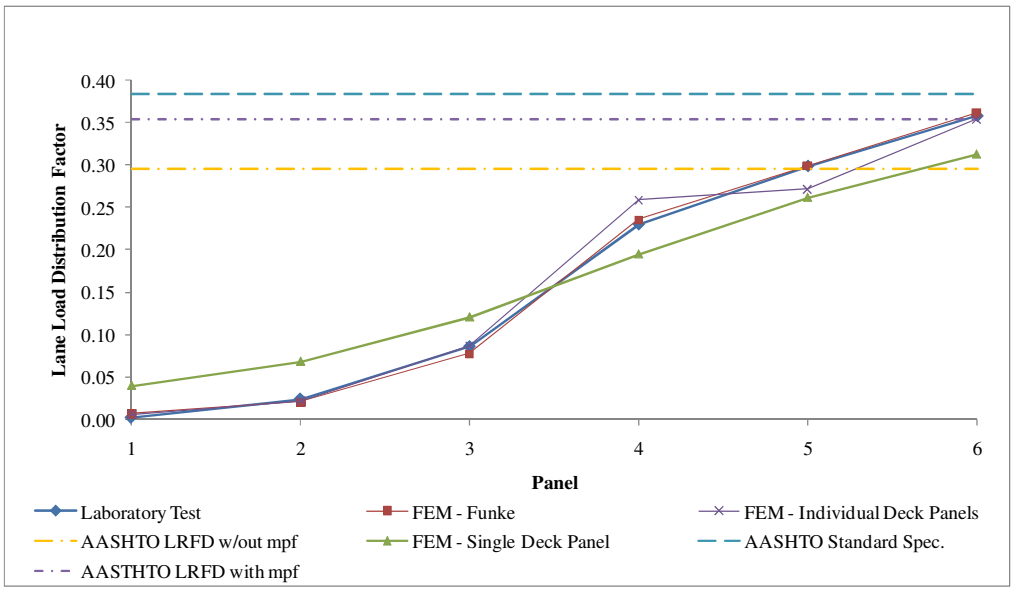

Figure 59. Laboratory Test Bridge ITE6-A, Lane Load Distribution Results

A summary of the controlling live load distribution factors, from above, are provided in Table 30. From the live load distribution factor results of the laboratory bridge, one can notice the bridge that the deck of the bridge does not behave as a single panel structure due to the large differential displacement between the deck panels. This was expected due to the large spacing between the stiffener beams, absence of a wearing surface, and small friction between the deck panels. Additional finite element trials will be performed to investigate the effects of the stiffener beam spacing, stiffener beam size, and influence of friction on the laboratory bridge above.

Table 30. Laboratory Bridge, Live Load Distribution Factors

Exterior Panel Live Load Distribution Results	
Laboratory Test =	0.359
FEM - Individual Deck Panels =	0.368
FEM - Single Deck Panel =	0.311
AASHTO Standard Spec. =	0.384
AASHTO LRFD Spec. with mpf =	0.355
AASHTO LRFD Spec. without mpf =	0.296

Affects of stiffener beam properties and spacing

Using the laboratory test bridge, a parametric study was conducted to investigate the influence of the stiffener beam properties and spacing on the live load distribution results. Utilizing the load configuration shown in Figure 57, the controlling live load distribution values were determined for the exterior panel. These results are listed in Table 31. One can observe how the load is distributed from the exterior to the adjacent panels as the number of stiffeners is increased. However, increasing the number of stiffener beams alone does not provide a result which fully converges to the results obtained assuming the deck panel acts as a single deck panel. Therefore, for the single panel action to occur a combination of swelling and close stiffener beam spacing must be present.

Table 31. Stiffener Beam Parametric Study

Lane Load Distribution Factor	
AASHTO Standard Spec.	0.384
ASHTO LRFD w/out mpf	0.296
ASHTO LRFD with mpf	0.355
No Stiffener Beam	0.500
1 Stiffener Beam	0.368
2 Stiffener Beams	0.360
4 Stiffener Beams	0.351
(2x) Stiffener Beam Depth	0.356
Single Deck Panel	0.311

The influence of the swelling on the behavior of the bridge is difficult to quantify. As the bridge panels swell, additional load is transferred to adjacent panels through friction forces. Similar to the table above, additional trials were performed modifying the interaction of the deck panels. When modeling the bridge with the individual deck panels, the nonlinear spring elements connecting the deck panels were assigned large coefficient of friction and stiffness values. The controlling lane load distribution results, for the controlling exterior deck panel, are shown in Table 32.

Table 32. Stiffener Beam Parametric Study Including Deck Panel Interaction

Lane Load Distribution Factor	
AASHTO Standard Spec.	0.384
ASHTO LRFD w/out mpf	0.296
ASHTO LRFD with mpf	0.355
No Stiffener Beam	0.408
1 Stiffener Beam	0.355
2 Stiffener Beams	0.341
4 Stiffener Beams	0.331
(2x) Stiffener Beams Depth	0.341
Single Deck Panel	0.311

Comparing the results from Tables 31 and 32, one can observe the influence of the deck panel interaction with multiple stiffener beam arrangements. Notice from Table 32, there is a seven percent difference between the single deck panel results and results utilizing four stiffener beams including the deck panel interaction. To further increase the deck panel interaction one could provide a transverse post-tensioning system. This would aid in the distribution of load and assure the panelized system behaves similar to a single deck panel structure.

Multiple vehicle loads

The above analyses focus on single design truck loads. From these analyses, one can note the in-service bridges perform similar to a single panel structure and compared reasonably well to the 2005 AASHTO LRFD live load distribution provisions. Accurate simplified single lane load equivalent strip width equations are necessary, but for many bridges the design will be controlled by a multiple lane load condition. To further explore the AASHTO LRFD equivalent strip width equations, the multiple lane load case will be reviewed for two bridges. The bridges will be modeled as a single deck panel, similar in behavior to the in-service bridges. The effects from the asphalt wearing surface and edge stiffening effects from guardrails will be neglected.

The first bridge analyzed with two vehicle loads had a span length of 26’-0” and a clear

width of 24’-0”, similar in dimensions to the laboratory test bridge. The deck panels were 4’-0” wide and had a depth of 10.72 inches. Three stiffener beams were spaced at 6’-6”, each having a depth of 4.5 inches and a width of 6.75 inches. As previously stated, the bridge was modeled as a single deck panel behaving similar to the in-service bridges. The single deck panel was divided into six sections, each having a tributary width of 4’-0”. The average stress and moment results for each of the six sections was used to determine the equivalent strip width values, similar to a slab-girder bridge. The controlling beam-line moment of 275 ft-kips was due to the AASHTO LRFD tandem loading condition shown in Figure 60 below. The results are provided in Table 32 below.

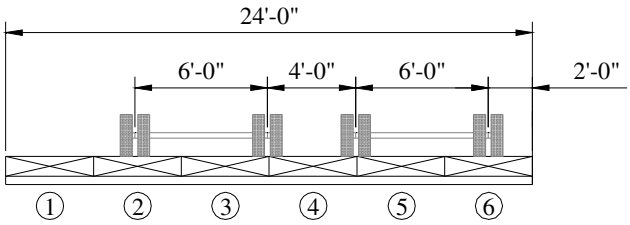

Figure 60. AASHTO LRFD Transverse Tandem Truck Loading

From Table 33, one can observe the controlling equivalent strip width value occurs at panel six. Using Table 24, the controlling AASHTO LRFD equivalent strip width values is 10.0 feet. The AASHTO LRFD equivalent strip width value is within a five percent difference of the controlling result, 10.5 feet, provided in Table 33.

Table 33. Multiple Lane Load Results

Panel Number	Stress psi	Moment ft-kips	Equiv. Width E (ft)
1	706.61	54.13	20.32
2	1002.98	76.84	14.32
3	1095.64	83.94	13.10
4	1285.36	98.47	11.17
5	1283.70	98.35	11.18
6	1367.50	104.77	10.50
Sum	6741.79	516.50	

The second bridge analyzed with two vehicle loads was East Main Street Bridge. This in-service bridge was arbitrarily selected from above. As previously stated, the bridge was modeled as a single deck panel. Edge stiffening effects were neglected, modeling the clear width of the bridge. The single deck panel was divided into eight sections, the inner sections had a tributary width of 4'-6" and the two outer sections had a tributary width of 3'-5". The average stress and moment results for each of the eight sections were used to determine the equivalent strip width values, similar to a slab-girder bridge. The controlling beam-line moment of 331 ft-kips was due to the AASHTO LRFD tandem loading condition shown in Figure 61 below.

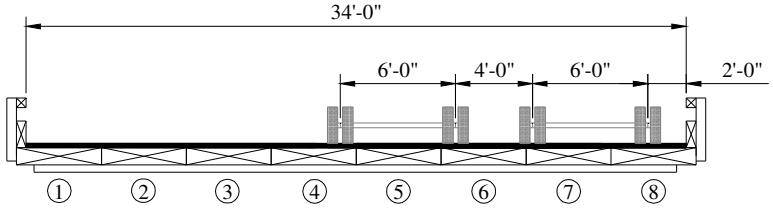

Figure 61. AASHTO LRFD Tandem Truck Loading, East Main Street Bridge

From Table 34, one can observe the controlling equivalent strip width value occurs at panel eight. Using Table 24, the controlling AASHTO LRFD equivalent strip width values is 10.6 feet. The AASHTO LRFD equivalent strip width value is within a five percent difference of the controlling result, 10.22 feet, provided in Table 34.

Table 34. Multiple Lane Load Results, East Main Street Bridge

Panel Number	Stress psi	Moment ft-kips	Equiv. Width E (ft)
1	108.48	12.40	93.68
2	159.42	23.43	63.74
3	271.77	39.95	37.39
4	521.12	76.60	19.50
5	703.69	103.44	14.44
6	877.06	128.93	11.59
7	907.26	133.37	11.20
8	993.96	113.64	10.22
Sum	4542.76	631.77	

Conclusions

This research involved the evaluation of the existing live load distribution equations for longitudinal glued-laminated timber deck bridges provided in the 2005 AASHTO LRFD Bridge Design Specification. This was accomplished by using analytical finite element models, which were validated with test data from in-service and laboratory bridges. The test data consisted of deflections and live load distribution factors for each panel.

Analytical finite element models were developed utilizing ANSYS [3], a general purpose finite element program. The finite element model utilized bilinear solid “brick” elements to model the timber deck panels as well as the stiffener beams. The program provided the user the option to model the bridge as one single deck panel or as having individual deck panels. When modeling the individual deck panels, the program allowed the user to adjust the panel-to-panel interaction with spring elements. Compression only spring elements were utilized to idealize the interface between the panels and the stiffener beam. Additionally, tension-compression spring elements were utilized to model the through bolt, or aluminum bracket, connection of the stiffener beam to the deck panels. Utilizing the ANSYS parametric design language (APDL) greatly simplified the user input, reducing the modeling time required by the user.

Four in-service bridges were analyzed with the finite element program described above. The four in-service bridges behaved as a single deck panel. The single deck panel behavior of the in-service bridges is due to the stiffener beam spacing and swelling of the deck panels. Additionally, edge stiffening was also observed from the in-service bridge results, affecting both the deflection and load distribution values. Based on the analytical and in-service bridge results above, one can conclude the 2005 AASHTO LRFD live load distribution provisions for longitudinal glued-laminated timber bridges are acceptable. This was observed for both the single and multiple lane loading conditions.

One laboratory test bridge was analyzed with the finite element program described above. The laboratory test bridge allows one to study the behavior of the longitudinal glued-laminated timber deck panel bridge without the influence of swelling and edge stiffening effects from the guardrails. The individual deck panel model allows one to adjust fiction interface between the deck panels. When modeling the bridge with the individual deck panels, the nonlinear spring elements connecting the deck panels were assigned negligible coefficient of friction and stiffness values, allowing the deck panels to slide freely.

The AASHTO LRFD specification reduced the required minimum stiffener beam spacing provided in the AASHTO Standard specification from ten feet to eight feet or less. No changes were made to the required stiffness of the stiffener beam, 80,000 kip-in^2. The in-service bridges had stiffener beam spacing's of 6'-0" or 7'-6" on-center meeting the AASHTO LRFD requirements. A parametric study was conducted on the laboratory bridge to investigate, stiffener beam spacing, stiffener beam depth, and panel-to-panel interaction. With large panel-to-panel interaction and stiffener beams spaced at approximately 5'-0", the individual deck panel model produced results similar to the single deck panel model. Modifying the stiffness of the

stiffener beam had minimal influence on the distribution of load. All of the longitudinal deck panel bridges analyzed in this report utilized through-bolts to connect the deck panels to the deck panels. The aluminum bracket connection was not investigated in this report.

Recommendations

Based on the analytical finite element results and the comparison of the results above, the following can be recommended:

1. The AASHTO LRFD equivalent strip width equations assume the panelized structure behaves as a single panel bridge. This assumption appears to be valid based on the performance of the in-service bridges. To assure the panelized structure performs as a single panel; additional research should be performed on the spacing of the stiffener beams, swelling of the deck panels, and the influence of edge stiffening.
2. The existing AASHTO LRFD equivalent strip width equations compared well to the in-service bridges and the analytical results. At times the single lane equivalent strip width equation was not conservative. However, with the inclusion of the single lane multiple presence factor, the AASTHO LRFD Specification will provide conservative results. It is recommended that no modifications be made to the multiple presence factor for bridges with lower ADTT values.
3. For newly constructed longitudinal glued-laminated timber deck bridges, their behavior will be similar to the laboratory bridge analyzed in this report. One should consider using the AASHTO Standard Specification load distribution factors for newer bridges that have not undergone swelling and do not have guard rails.

REFERENCES

[1] AASHTO. 1996. Standard Specifications for Highway Bridges, Sixteenth Edition. Washington, DC: American Association of State Highway and Transportation Officials.

[2] AASHTO LRFD. 2005. LRFD Bridge Design Specifications. Washington, DC: American Association of State Highway and Transportation Officials.

[3] ANSYS. 1992. User's manual for revision 5.0, Procedures. Houston: PA, Swanson Analysis Systems, Inc.

[4] Barker, R. M., Puckett, J. A. Design of Highway Bridges Based on AASHTO LRFD Bridge Design Specifications. New York, NY: Wiley and Sons, Incorporated.

[5] Cai, C.S. 2005. Discussion on AASHTO LRFD Load Distribution Factors for Slab-on-Girder Bridges. Practice Periodical on Structural Design and Construction, Vol 10, No. 3, August 1. American Society of Civil Engineers.

[6] Cha, H. 2004. Analysis of Glued-Laminated Timber Girder Bridges. Masters Thesis. Ames, IA: Iowa State University.

[7] Forest Products Laboratory. 1999. Wood Handbook, wood as an engineering material. Madison, WI: United States Department of Agriculture, Forest Service, Forest Products Laboratory.

[8] Hosteng, T. K. 2004. Live Load Deflection Criteria for Glued Laminated Structures. Masters Thesis. Ames, IA: Iowa State University.

[9] Kurian, A. V. 2001. Finite Element Analysis of Longitudinal Glued-laminated Timber Deck and Glued-laminated Timber Girder Bridges. Masters Thesis. Ames, IA: Iowa State University.

[10] Lee, P.H.L., Wacker, J.P. 2000. Standard Plans for Timber Highway Structures. National Conference on Wood Transportation Structures, Forest Products Laboratory, USDA Forest Service, Madison, WI.

[11] Pucket, J. A., et.al. 2006. Simplified Live Load Distribution Factor Equations. NCHRP Report for 12-62. TRB, National Research Council, Washington, D.C.

[12] Wipf, T. J., et.al. 2004. Live Load Deflection of Timber Bridges, 1. Badger Creek Glued-Laminated Girder Bridge. Ames, IA: Iowa State University, Bridge Engineering Center.

[13] Wipf, T. J., et.al. 2004. Live Load Deflection of Timber Bridges, 7. Chambers County Glued-Laminated Girder Bridge. Ames, IA: Iowa State University, Bridge Engineering Center.

[14] Wipf, T. J., et.al. 2004. Live Load Deflection of Timber Bridges, 6. Russellville Glued-Laminated Girder Bridge. Ames, IA: Iowa State University, Bridge Engineering Center.

[15] Wipf, T. J., et.al. 2004. Live Load Deflection of Timber Bridges, 5. Wittson Glued-Laminated Girder Bridge. Ames, IA: Iowa State University, Bridge Engineering Center.

[16] Yousif, Z., Hindi, R. 2005. Discussion on AASHTO LRFD Load Distribution Factors for Slab-on-Girder Bridges. Journal of Bridge Engineering, Vol 12, No. 6, November 1. American Society of Civil Engineers.

[17] Wolfram Research, "Affine Transformation," http://mathworld.wolfram.com/AffineTransformation.html, 2004.

[18] Zokaie T., et.al. 1993. Distribution of Wheel Loads on Highway Bridges. NCHRP Report 12-26 TRB, National Research Council, Washington, D.C.

[19] Funke, R. W. 1986. Behavior of Longitudinal Glued Laminated Timber Deck Bridges. Masters Thesis. Ames, IA: Iowa State University.

[20] Sanders, W. W., et.al. 1985. Load Distribution in Glued Laminated Longitudinal Timber Deck Highway Bridges. Report No. ERI-85441. Iowa State University, Ames, Iowa.

[21] Wipf, T. J., et.al. 2004. Live Load Deflection of Timber Bridges, 10. Angelica Creek Glued-Laminated Panel Bridge. Ames, IA: Iowa State University, Bridge Engineering Center.

[22] Wipf, T. J., et.al. 2004. Live Load Deflection of Timber Bridges, 9. East Main Street Glued-Laminated Panel Bridge. Ames, IA: Iowa State University, Bridge Engineering Center.

[23] Wipf, T. J., et.al. 2004. Live Load Deflection of Timber Bridges, 11. Bolivar Glued-Laminated Panel Bridge. Ames, IA: Iowa State University, Bridge Engineering Center.

[24] Wipf, T. J., et.al. 2004. Live Load Deflection of Timber Bridges, 12. Scio Glued-Laminated Panel Bridge. Ames, IA: Iowa State University, Bridge Engineering Center.

[25] Hale, C. Y., 1978. Stiffened Longitudinal Decked Bridge – Evaluation of Stiffener Hardware. Report No. 045-16093, Weyerhaeuser Co., Tacoma.

[26] Gilham, P. C., Ritter, M. 1994. Load Distribution in Longitudinal Stringer-Transverse Deck Timber Bridges. Madison, WI: United States Department of Agriculture, Forest Service, Forest Products Laboratory.

ACKNOWLEDGMENTS

The author of this report wishes to thank the United States Department of Agriculture/Forest Service/Forest Products Laboratory for sponsoring this research project. Additional recognition is given to everyone who contributed to the research presented and to the completion of this report. With special thanks to my major professors Dr. Fouad S. Fanous and Dr. Terry J. Wipf for their extensive help, involvement, co-operation, and enthusiasm throughout the project. The author also thanks Mr. Michael A. Ritter of the Forest Products Laboratory for providing additional input required for this report.